Molecular Therapy
Nucleic Acids
Original Article

Rescue of the disease-associated phenotype in CRISPR-corrected hiPSCs as a therapeutic approach for inherited retinal dystrophies

Laura Siles[1] and Esther Pomares[1]

[1]Departament de Genètica, Institut de Microcirurgia Ocular, IMO Grupo Miranza, 08035 Barcelona, Spain

Inherited retinal dystrophies (IRDs), such as retinitis pigmentosa and Stargardt disease, are a group of rare diseases caused by mutations in more than 300 genes that currently have no treatment in most cases. They commonly trigger blindness and other ocular affectations due to retinal cell degeneration. Gene editing has emerged as a promising and powerful strategy for the development of IRD therapies, allowing the permanent correction of pathogenic variants. Using clustered regularly interspaced short palindromic repeats (CRISPR)-Cas9 and transcription activator-like effector nucleases (TALEN) gene-editing tools, we precisely corrected seven hiPS cell lines derived from IRD patients carrying mutations in *ABCA4*, *BEST1*, *PDE6A*, *PDE6C*, *RHO*, or *USH2A*. Homozygous mutations and point insertions/deletions resulted in the highest homology-directed repair efficiencies, with at least half of the clones repaired properly without off-target effects. Strikingly, correction of a heterozygous pathogenic variant was achieved using the wild-type allele of the patient as the template for DNA repair. These results suggest the unexpected potential application of CRISPR as a donor template-free strategy for single-nucleotide modifications. Additionally, the corrected clones exhibited a reversion of the disease-associated phenotype in retinal cellular models. These data strengthen the study and application of gene editing-based approaches for IRD treatment.

INTRODUCTION

Inherited retinal dystrophies (IRDs) are a group of heterogeneous eye diseases that cause vision loss due to impaired function or degeneration of photoreceptors or retinal pigment epithelium (RPE) cells.[1] They are rare disorders, affecting 1 in 4,000 individuals with 5.5 million patients worldwide.[2,3] IRDs follow autosomal dominant or recessive, or X-linked inheritance patterns caused by mutations in approximately 300 genes.[1,4–6] Despite the development of novel therapeutic strategies, still no treatment strategy currently exists to cure or stop disease progression in the vast majority of IRDs, except for specific genes and mutations.[4,7]

Clinical manifestations in IRD are diverse depending on the gene and cell type affected, and can be syndromic, generating a broad phenotypic diversity.[1,4] The most common one is retinitis pigmentosa, which is characterized by the degeneration of photoreceptors triggering several visual complications and blindness.[8] It is considered one of the most genetically heterogeneous disorders in humans with reported mutations in more than 100 genes.[1,4] Conversely, Stargardt disease is caused by pathogenic variants only in the *ABCA4* gene, and is responsible for 12% of IRD-related blindness.[9] Patients with achromatopsia also suffer from photoreceptor degeneration, but in this case individuals are deprived of color vision.[10] Other forms include Best disease, Leber congenital amaurosis (LCA), or Usher syndrome.[1]

The management of IRD is complex and relies on genetic diagnosis and counseling, together with ophthalmologic follow-up, to improve visual quality and reduce patient symptomatology. Many clinical trials are ongoing. However, owing to the broad spectrum of IRD-related genes and mutations, therapeutic approximations are diverse and complex. Moreover, the different clinical stages of disease progression could help determine the most suitable treatment. In particular, gene therapy is the most explored approximation for therapeutic use, for example Luxturna gene therapy for patients with autosomal recessive *RPE65* mutations in LCA.[11,12] Gene augmentation represents one of the most desired treatment modalities for gene therapy, such as in *CNGA3* and *CNGB3* trials in patients with achromatopsia.[13,14] Nevertheless, this is not appropriate for gain-of-function mutations or in cases of toxicity of the protein products. Additionally, the limited cargo capacity of adeno-associated viruses used in gene therapy could be challenging for large genes such as *ABCA4*.[15,16]

Other emerging approximation alternatives to viral-based technologies are being studied, showing promising results, such as optogenetics, antisense oligonucleotides,[17] or nanoparticles.[18,19] Moreover, cell therapy is a key strategy for the replacement of damaged tissue.[20] Noteworthy, stem cell-based therapy from allogeneic or autologous donors has demonstrated encouraging results in RPE cell transplants.[21]

Gene editing has emerged as an important tool for the modification of the DNA, with a special interest in translational medicine for its

Received 30 April 2024; accepted 6 February 2025;
https://doi.org/10.1016/j.omtn.2025.102482.

Correspondence: Esther Pomares, Departament de Genètica, Institut de Microcirurgia Ocular, IMO Grupo Miranza, 08035 Barcelona, Spain.
E-mail: esther.pomares@imo.es

Published by Elsevier Inc. on behalf of The American Society of Gene and Cell Therapy.
This is an open access article under the CC BY-NC-ND license (http://creativecommons.org/licenses/by-nc-nd/4.0/).

ability to permanently correct pathogenic variants avoiding re-administration.[7,22–24] Nonetheless, some important issues with respect to precision, efficiency, safety, loading, and *in vivo* delivery still exist.[16,25] However, efforts are being made to tackle all these concerns for its application in personalized medicine.[16,24–26] Recently, the EDIT-101 clinical trial has been approved for the removal of an aberrant splice donor in *CEP290* (c.2991 + 1655A>G) through subretinal delivery of the clustered regularly interspaced short palindromic repeats (CRISPR)-Cas9 system using an AAV5 vector in LCA patients.[27,28] Also other genetic disorders, including cancer,[29–31] Duchenne muscular dystrophy[32] or viral infections,[33–35] are taking advantage of genome editing as a therapeutic strategy.

Zinc finger nucleases and transcription activator-like effector nucleases (TALENs) were the first-generation nucleases used for gene editing; however, they appeared to be complex and expensive.[36] Decisively, the advent of CRISPR-associated nuclease Cas9 technology marked an important improvement in gene-editing tools due to its precision, ease, and potential.[23,37] Currently, the most used technology is, by far, CRISPR, despite TALENs are also appreciated because of their high specificity.[37,38] In both technologies, the genomic regions of interest are targeted by either primer sequences in TALENs or by a single guide RNA (sgRNA) in CRISPR-Cas9, which needs to be just beside the protospacer-adjacent motif (PAM)—the tri-nucleotide "NGG" in case of Cas9 from *Streptococcus pyogenes*.[23]

Both TALEN and CRISPR-Cas9 rely on cellular repair mechanisms to restore DNA double-strand breaks (DSBs) generated by FokI or Cas9 nucleases, respectively.[24,39–41] This repair is predominantly performed by two major error-prone systems: the non-homologous end-joining (NHEJ) and microhomology-mediated end-joining (MMEJ) pathways.[42] NHEJ joins the broken DNA ends, while MMEJ uses short homologous sequences near the DSB for its repair.[43] Moreover, DNA repair machinery has also a mechanism to precisely repair DSB, named homology-directed repair (HDR), which needs a homologous DNA template.[40,44–46]

Specifically, the HDR mechanism can follow homologous recombination (HR) or single-strand template repair (SSTR).[43–48] The HR mechanism uses a sister chromatid or a homologous chromosome as the template,[35,44,47] while SSTR needs a homologous single-stranded DNA for gene correction, such as a single-stranded oligodeoxynucleotide (ssODN).[40,45,47–49] Although HDR would be the preferred mechanism for proper gene-editing assays, NHEJ is the most active pathway in mammalian and non-dividing cells, which commonly repair DNA by introducing small insertions and deletions.[42,45,47,50–53] Additionally, it has been extensively reported that NHEJ is the favored mechanism to repair DNA lesions after Cas9-induced DSBs.[44,45,47] Thereby, drugs to enhance the HDR pathway instead of NHEJ are largely used in gene correction assays.[26,42,44]

In this study, we report the efficient and precise correction of point mutations in seven induced pluripotent stem cell (hiPSCs) lines derived from patients with IRD. The percentage of properly edited clones ranges from 3% to more than 70% of the screened clones, depending on the gene, pathogenic variant, and technology used. Specifically, homozygous and small insertions/deletions exhibited the highest HDR efficiencies. Moreover, the distance between the DSB and the pathogenic variant and sgRNA specificity decisively influenced gene-editing outcomes. Surprisingly, in some gene-editing assays of hiPS cell lines from heterozygous carriers, the pathogenic variant was corrected using the wild-type allele of the patient as the template for repair. Finally, the repaired clones exhibited reversion of the IRD-associated phenotype in retinal cell models compared with mutant hiPSCs, indicating a potential rescue of the diseased condition.

Most IRDs are caused by point mutations,[54] like the ones studied in this article. Hence, the precise correction of pathogenic variants in patient-derived iPSCs using gene-editing technologies is a promising therapeutic approach for retinal dystrophies. The results presented here support and broaden the application of gene editing as a future prospect for IRD treatment.

RESULTS

Design and validation of the optimal sgRNA and TALEN guides for targeting IRD-related pathogenic variants

IRDs are mainly caused by single point mutations or small insertions/deletions[55] that can be corrected by gene editing using an ssODN as a repair template. For that purpose, we aimed to correct seven iPS cell lines derived from patients with different retinal disorders. Specifically, patients with Stargardt disease, Best disease, achromatopsia, or retinitis pigmentosa. All hiPS cell lines carried previously described heterozygous or compound-heterozygous point mutations in *ABCA4, BEST1, PDE6A, RHO,* or *USH2A* genes, except in the patient with achromatopsia who harbored a homozygous missense change in *PDE6C* (listed in Table 1). For compound-heterozygous carriers, we selected only one pathogenic variant for correction because of its recessive behavior (asterisks in Table 1).

We focused on CRISPR and TALEN technologies because of their efficacy and precision, as well as their low ratio of off-target effects, respectively. We designed several sgRNAs for CRISPR-Cas9 and one TALEN mRNA pair for each selected pathogenic variant in the seven hiPS cell lines (schematized in Figures 1A and 1B; Table S1). Moreover, we designed an ssODN specific for each mutation and technology considering some important parameters to enhance HDR-mediated repair, such as the length of the left and right homologous arms, the location of the DSB that should be centered, and the incorporation of phosphorothioate modifications at the ends of the template.[53,66] Importantly, the ssODN also harbored a synonymous nucleotide substitution in the PAM sequence to avoid Cas9 re-cutting in the case of successful knockin in CRISPR experiments[66,67] (nucleotides in blue in Table S2).

DNA cleavage analyses showed a higher efficacy of sgRNAs than TALENs except when targeting the mutation in *USH2A*, in which cleavage was similar for both technologies (Figures 1A and 1B; Table S1). The Cas9-mediated DSB cleavage efficiency ranged from

Table 1. hiPS cell lines derived from patients affected with IRD

Patient ID	hiPS cell line	IRD	Gene	Zygosis	Allele	Variant[a]	Protein change
ABCA4_A	FRIMOi003-A	Stargardt disease	*ABCA4*	comp-het	1	c.4253 + 4C>T[a,56]	Splicing
					2	c.6089G>A[57]	p.Arg2030Gln
ABCA4_B	FRIMOi004-A	Stargardt disease	*ABCA4*	comp-het	1	c.3211_3212insGT[a,58]	p.Ser1071CysfsTer14
					2	c.514G>A[59]	p.Gly172Ser
					2	c.2023G>A[60]	p.Val675Ile
					2	c.6148G>C[58]	p.Val2050Leu
BEST1	FRIMOi006-A	Best disease	*BEST1*	het	1	c.229C>T[a,61]	p.Pro77Ser
					2	–	–
PDE6C	FRIMOi007-A	Achromatopsia	*PDE6C*	homo	1	c.1670G>A[a,62]	p.Arg557Gln
					2	c.1670G>A[a,62]	p.Arg557Gln
PDE6A	FRIMOi001-A	Retinitis pigmentosa	*PDE6A*	comp-het	1	c.305G>A[63]	p.Arg102His
					2	c.1268delT[a,63]	p.Leu423Ter
RHO	FRIMOi005-A	Retinitis pigmentosa	*RHO*	het	1	c.644C>T[a,64]	p.Pro215Leu
					2	–	–
USH2A	FRIMOi002-A	Retinitis pigmentosa	*USH2A*	comp-het	1	c.2209C>T[a,65]	p.Arg737Ter
					2	c.8693A>C[a,65]	p.Tyr2898Ser

[a]Selected pathogenic variant for gene editing.

0% to approximately 55% (Figure 1A). However, we obtained considerable cleavage by TALENs only with guides targeting *BEST1, PDE6C,* and *USH2A* mutations (Figure 1B). Notably, sgRNAs with a GC content between 46% and 60% display the highest cleavage efficiencies, suggesting a correlation with their ability to induce DSB, but not with TALEN mRNA pairs (Figure S1A). Noteworthy, we did not study sgRNAs with GC content higher than 60%.

Consequently, sgRNAs or TALEN mRNAs that were unable to induce DSB or exhibited low DNA cleavage were discarded for the gene-editing assays. Finally, we selected one sgRNA harboring the pathogenic variant to increase allele specificity, with the lowest distance between the DSB and the mutation for each mutation in the seven hiPS cell lines (green guides in Table S1).

Efficient HDR correction of pathogenic variants in hiPSCs from IRD patients without off-target effects

Single-nucleotide gene editing relies on the precise correction of single or small nucleotide changes by HDR mechanisms.[44,46,48,53] To that end, we electroporated either sgRNA/Cas9 or TALEN mRNA pairs, together with the corresponding ssODNs (summarized in Table S2) in patient-derived iPSCs. Following electroporation, the cells were cultured with L755507 activator, M3814 inhibitor, and Y-27635 ROCK inhibitor to improve HDR repair and cell survival. Finally, single colonies were cultured and Sanger sequenced to assess gene-editing outcomes (Figure 1C).

Sequencing analysis revealed substantial differences in gene-editing efficiency based on the type of technology, mutation, zygosity, and genomic region, resulting in different percentages of properly corrected clones without on-target abnormalities in each assay (Figure 1D; Table 2). After CRISPR-Cas9-mediated gene editing, we successfully corrected the pathogenic variant in all iPS cell lines, except for FRIMOi002-A (*USH2A* c.2209C>T), which was repaired using TALENs (Figure 1D). Notably, both sgUSH2A_2 and talUSH2A_1 induced DNA DSB with moderate efficiency (<10%) (Table S1). However, we could not obtain repaired clones of FRIMOi006-A (*BEST1* c.229C>T) or FRIMOi007-A (*PDE6C* c.1670G>A) using TALENs (Figure 1D). Noteworthy, hiPSCs after TALEN electroporation exhibited poorer overall cell survival compared with CRISPR-Cas9-treated cells.

Remarkably, the highest HDR efficiencies with the absence or lowest ratios of on-target effects were found in gene-editing assays targeting the di-nucleotide insertion, the single-nucleotide deletion, and the homozygous mutation (*ABCA4* c.3211_3212insGT, *PDE6A* c.1268delT, and *PDE6C* c.1670G>A, respectively) (Figures 1E and 1F). In the majority of cases, the percentages of on-target aberrations were <25%, and <40% in all assays (Figure 1F). Notably, we did not obtain on-target anomalies when correcting for either of the *ABCA4* mutations (c.4253 + 4C>T and c.3211_3212insGT) (Table 2). Moreover, the best knockin results were found in assays with sgRNAs that had the shortest distances between the DSB and the targeted mutation (Figure S1B).

Corrected clones generated using CRISPR or TALEN showed hiPSC-like cellular morphology and proliferation rates similar to those of the parental clones (Figure 1G). In addition, we found no significant differences in the expression of stemness-related genes between clones (Figure S1C and reported previously[68,69]). Likewise, they shared the

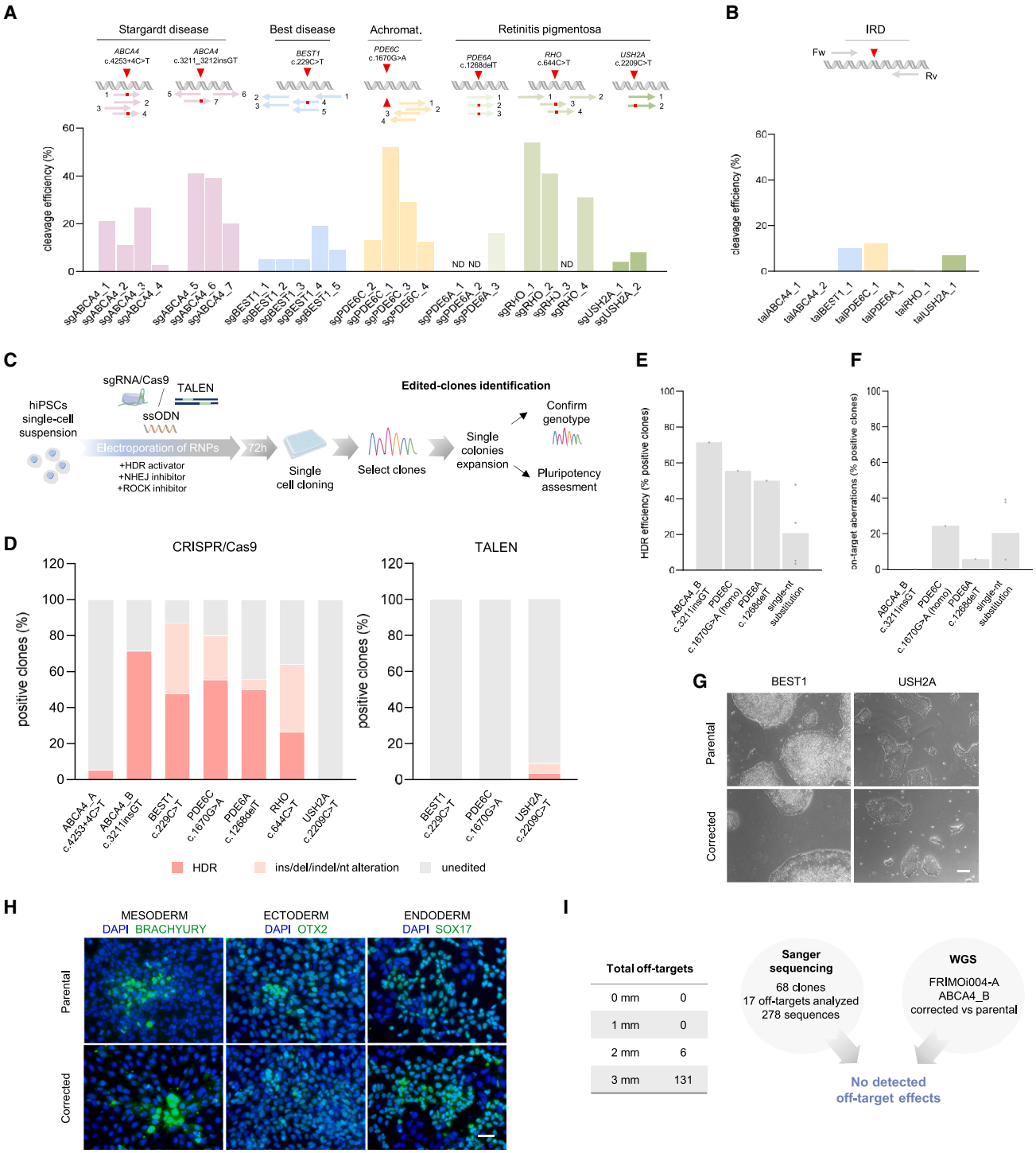

Figure 1. Efficient HDR correction of pathogenic variants in hiPSCs from IRD patients without off-target effects

(A) *Top*: Schematic representation of sgRNAs designed for each pathogenic variant for gene editing in each hiPS cell line. *Bottom*: Cleavage efficiencies of the sgRNAs ("ND" means not detected). (B) As in (A) but for TALENs. (C) Gene-editing assay overview. The figure was partly generated using Servier Medical Art, provided by Servier, licensed under a Creative Commons Attribution 3.0 Unported license. (D) Gene-editing results for each pathogenic variant. HDR percentages indicate corrected clones without

(legend continued on next page)

same ability to differentiate into the three embryonic germ layers and into retinal 3D models, named organoids, demonstrating the preservation of pluripotency after gene editing (Figures 1H, S1D, and S1E).

Gene editing can cause undesired genomic alterations because of error-prone repair or binding of the guides to off-target regions.[46,53,70] For off-target assessment, we analyzed all predicted regions with two mismatches in sequence homology, and most of the predicted homologous loci presenting three mismatches corresponding to exonic or intronic regions. In more than 250 off-target sequences analyzed by Sanger sequencing, undesired genomic alterations were not detected in the 68 repaired clones screened (Figure 1I; Table 3), suggesting that two or more mismatches in sequence homology prevented the binding of the sgRNA to off-target regions. Additionally, we performed whole genome sequencing (WGS) analysis of one corrected and one parental FRIMOi004-A clone and found no genomic abnormalities derived from the CRISPR-Cas9 gene editing, as previously reported (Figure 1I).[68]

Altogether, these results indicate the precise HDR correction of IRD-related point mutations using CRISPR-Cas9 and TALEN technologies for several types of mutations and different genes. The highest knockin results were achieved when targeting homozygous or small ins/dels by CRISPR-Cas9, between 50% and 70% of properly corrected clones without on- and off-target defects, and were also associated with the sgRNAs exhibiting the shortest distances between the DSB and the mutation. Although TALEN-mediated gene editing was less efficient, we achieved successful pathogenic variant repair in FRIMOi002-A (c.2209C>T *USH2A*) but not by CRISPR-Cas9.

Precise HDR correction of pathogenic variants by using the endogenous sister chromatid

Using CRISPR gene-editing assays for the repair of heterozygous mutations, we obtained a few clones that exhibited pathogenic variant correction but did not harbor the PAM mutation. Remarkably, we also observed edited clones carrying the pathogenic variant in homozygosis instead of heterozygosis or corrected (Figure S2A). This observation indicates DNA cleavage of the wild-type allele and DSB resolution by incorporating the mutation, which could not occur if ssODNs were used as the template for repair. HDR mechanisms can use exogenous (ssODN in the SSTR pathway) or endogenous homologous sequences, such as the sister chromatid (HR pathway) (Figure 2A).[44,45,71]

This prompted us to study whether we had obtained the undesired cut and HDR repair of the wild-type allele in some gene-editing assays. Specifically, cutting of the wild-type allele would result in: (1) clones carrying the pathogenic variant and PAM mutation in heterozygosis (SSTR repair), or (2) clones with the pathogenic variant in homozygosis (HR repair), as shown in Figure 2B. Significantly, we observed these two genotypes only when using sgRNAs harboring one mismatch in sequence homology with the wild-type allele, but not when using sgRNAs with two or nine mismatches (Figure 2B, see sgABCA4_7 and sgPDE6A_3). Additionally, the results related to the correction of the pathogenic variant in the mutant allele showed the best HDR efficiencies when sgRNAs with at least two mismatches in sequence homology against the wild-type allele were used (Figure 2C). Altogether, these results suggest that better knockin efficiencies are associated with lower recognition of the wild-type allele, although it should be considered that the assays were performed in different hiPS cell lines and with different ssODNs, which could affect gene-editing efficiency.

Because heterozygous pathogenic variants are common in IRD,[4] precise and efficient gene editing should ideally target only the mutant allele to minimize undesired DNA modifications in the wild-type allele. To further analyze these findings, we focused on the gene editing of *BEST1* c.229C>T in FRIMOi006-A, which displayed similar ratios of SSTR- and HR-mediated repair (Figure 2D). We designed another sgRNA named sgBEST1_5, which harbors the same nucleotide change corresponding to the pathogenic variant but moved one position (nucleotides in blue in Figure 2E). This resulted in one mismatch against the wild-type allele and two mismatches against the mutant allele (dark blue asterisks in Figure 2E). Conversely, the previously designed guide, sgBEST1_4, showed perfect homology with the mutant allele and one mismatch with the wild-type allele (light blue asterisks in Figure 2E). As expected, sgBEST1_4 induced higher levels of DNA cleavage in FRIMOi006-A than sgBEST1_5, which worked better in wild-type hiPSCs because of sequence homology (Figures S2B and S2C).

We then compared the HDR efficiency for correction of the pathogenic variant in FRIMOi006-A using both sgRNAs. We obtained only one clone with the pathogenic variant corrected using sgBEST1_5, in contrast to more than 45% of successfully knocked-in clones obtained using sgBEST1_4 (Figure 2F). Significantly, we observed that sgBEST1_5 guide acted almost exclusively on the wild-type allele (Figure 2G), whereas the sgBEST1_4 guide mostly recognized the mutant allele (Figure 2F). Remarkably, the gene-editing assay performed with sgBEST1_4 did not generate clones with the pathogenic variant in homozygosis, whereas the assay performed with sgBEST1_5 resulted in 23.81% of clones with this genomic event (Figures 2H and S2D).

Notably, both BEST1 gene-editing assays were performed in the same hiPS cell line and using the same ssODN, indicating that the specificity

on-target defects from the total clones analyzed. (E) HDR ratios depending on the type of pathogenic variant. Single-nucleotide substitutions refer to mutations in ABCA4_A, BEST1, RHO, and USH2A patients. (F) As in (E) but quantification of on-target aberrations. (G) Bright field captures of hiPS clones after CRISPR-Cas9 (FRIMOi006-A) or TALEN (FRIMOi002-A) gene editing. Scale bar represents 200 μm. (H) Lineage differentiation analysis in FRIMOi002-A parental and corrected clones. Scale bar indicates 50 μm. (I) Table shows the total number of off-targets. *Right panel*: Scheme of Sanger sequencing screening results (in all hiPS cell lines) and of WGS analysis (in FRIMOi004-A).

Table 2. On-target gene-editing results

					HDR		Ins/del/indel/single-nt substitution	
Patient ID	Pathogenic variant	Zygosity	Guide ID	Clones	Clones	%	Clones	%
ABCA4_A	*ABCA4* c.4253 + 4C>T	het	sgABCA4_2	57	3	5.26	0	0
ABCA4_B	*ABCA4* c.3211_3212insGT	het	sgABCA4_7	42	30	71.43	0	0
BEST1	*BEST1* c.229C>T	het	sgBEST1_4	23	11	47.83	9	39.13
			sgBEST1_5	42	1	2.38	11	26.19
			talBEST1_1	36	0	0	0	0
PDE6C	*PDE6C* c.1670G>A	homo	sgPDE6C_4	45	25	55.56	11	24.44
			talPDE6C_1	22	0	0	0	0
PDE6A	*PDE6A* c.1268delT	het	sgPDE6A_3	52	26	50	3	5.77
RHO	*RHO* c.644C>T	het	sgRHO_4	53	14	26.42	20	37.74
USH2A	*USH2A* c.2209C>T	het	sgUSH2A_2	30	0	0	0	0
			talUSH2A_1	55	2	3.64	3	5.45

of the sgRNA for the mutant allele could decisively determine HDR gene-editing outcomes. In line with the previous results shown in Figure 2B, these data also suggest that the number of mismatches is crucial to avoid the wild-type allele DSB and HR repair that could generate clones carrying the pathogenic variant in homozygosis.

Pathogenic variant correction by using the wild-type allele as repair template in ssODN-free CRISPR-Cas9 gene-editing assay

The results showing DNA repair using the homologous sister chromatid prompted us to wonder if sgRNA-induced DSB without using an ssODN could be sufficient for correcting heterozygous pathogenic variants. Before further evaluating these findings, we first aimed to confirm the generation of homozygous pathogenic variants and ensure that we did not misidentify a potential heterozygous gross deletion as a result of NHEJ. Therefore, we analyzed the HR- and SSTR-corrected clones using karyotyping and long-read sequencing.

Karyotyping revealed no differences between the parental and corrected clones (Figure S3A). Notably, parental FRIMOi006-A hiPSCs harbored a balanced translocation (t(4; 22) (p14; q12)), as previously reported, which was also conserved in gene-edited clones.[46] Long-read sequencing resulted in 48 and 38 structural variants in SSTR- and HR-repaired clones, respectively (Tables S3 and S4). From these, approximately the 90% were in common with structural variants also detected in parental cells, and only 5% in the HR-edited clone were not found in the parental clone (Figure 3A). Furthermore, none of the structural variants were located in *BEST1* (Tables S3 and S4).

Taking advantage of the long-read sequencing results, we analyzed whether these detected structural variants could have arisen after gene editing as off-target effects. Each locus was amplified, run on a gel, and sequenced using Sanger sequencing (chromosomal positions are indicated in Table S4). To analyze the inversion, we designed two forward primers, one of which was located in the potentially inverted fragment, and one reverse primer (Table S7). PCR products of corrected clones revealed no bands corresponding to the predicted deletion and insertion and showed the same band pattern as the parental ones, including the inversion (Figures S3B–S3D). Additionally, we studied one deletion in chromosome 2 that was detected in the three samples and in wild-type hiPSCs, which was not found, indicating a false-positive result (Figure S3D). Importantly, these analyses revealed the absence of large on- or off-target effects due to CRISPR-Cas9 gene editing.

Subsequently, we performed the same gene-editing assay without ssODNs in the patients ABCA4_A, BEST1, PDE6A, and RHO (FRIMOi003-A, FRIMOi006-A, FRIMOi001-A, and FRIMOi005-A, respectively) (Figure 3B). Consequently, cell clones exhibiting gene editing of the pathogenic variant (either corrected or homozygous, depending on the cut allele) would indicate effective DSB repair using the endogenous sister chromatid.

We successfully corrected the c.229C>T *BEST1* pathogenic variant in more than 20% of the clones analyzed in the FRIMOi006-A cells (Figures 3C and S3E). This percentage of clones was similar to that achieved in the assay involving transfection with ssODNs (HR-mediated repair) (Figure 3C; Table S5). The corrected clones were also examined for other rare variants harbored by the patient, to ensure cell purity (Figure S3F). In contrast, iPSCs from patients ABCA4_A, PDE6A, and RHO failed to correct the mutations without ssODNs in the screened clones (Figure 3C). Nevertheless, in iPSCs from patient ABCA4_A we obtained a small number of clones with the pathogenic variant in homozygosis, indicating a wild-type allele cut and HR repair (Figure 3C). Notably, these three hiPS cell lines displayed lower ratios of the HR pathway than the BEST1 hiPSCs (Figure 3D). In addition, sgBEST1_4 had a shorter distance between the DSB and the pathogenic variant than the sgABCA4_3, sgPDE6A_3, and sgRHO_4 guides, which could also influence HR-mediated repair (Figure 3E), although we should still consider that this comparison is between assays performed in different cell lines.

Table 3. Off-target analysis results

Patient ID	Pathogenic variant	sgRNAs ID	Total off-targets		Exonic/intronic				Intergenic		
					Off-targets	Clones analyzed	Off-target effects		Off-targets	Clones analyzed	Off-target effects
ABCA4_A	*ABCA4* c.4253 + 4C>T	sgABCA4_2	7	1 mm	0	–	–	1 mm	0	–	–
				2 mm	0	–	–	2 mm	0	–	–
				3 mm	2	2	0	3 mm	5	0	–
ABCA4_B	*ABCA4* c.3211_3212insGT	sgABCA4_7	57	1 mm	0	–	–	1 mm	0	–	–
				2 mm	0	–	–	2 mm	1	33	0
				3 mm	17[a]	33	0	3 mm	39[a]	1	0
BEST1	*BEST1* c.229C>T	sgBEST1_4	16	1 mm	0	–	–	1 mm	0	–	–
				2 mm	1	6	0	2 mm	1	6	0
				3 mm	9	0	–	3 mm	5	0	–
PDE6C	*PDE6C* c.1670G>A	sgPDE6C_4	10	1 mm	0	–	–	1 mm	0	–	–
				2 mm	0	–	–	2 mm	0	–	–
				3 mm	6	14	0	3 mm	4	0	–
PDE6A	*PDE6A* c.1268delT	sgPDE6A_3	15	1 mm	0	0	0	1 mm	0	–	–
				2 mm	1	13	0	2 mm	0	–	–
				3 mm	11	0	–	3 mm	3	0	–
RHO	*RHO* c.644C>T	sgRHO_4	32	1 mm	0	–	–	1 mm	0		
				2 mm	0	–	–	2 mm	2	0	–
				3 mm	18	0	–	3 mm	12	0	–

[a]Some off-targets analyzed only by whole genome sequencing.

Next, we analyzed whether the absence of ssODNs could activate the NHEJ pathway. Although some clones displayed on-target genomic abnormalities (Figure S3E), the on-target aberration percentages were similar to those generated when providing ssODNs in the clones screened (Figure 3F).

Altogether, the results derived from these studies showed that gene-editing outcomes are highly influenced by the specificity of sgRNA and could be conditioned by the HDR pathway used for DSB repair. This study also demonstrated unexpected gene editing of the heterozygous *BEST1* c.229C>T mutation using CRISPR-Cas9 technology without ssODN. Furthermore, heterozygous mutations could benefit from the wild-type allele as a template for correction of the pathogenic variant upon sgRNA/Cas9-induced DSB.

HDR-corrected clones exhibit reversion of the mutant-associated phenotype in retinal cellular models

IRD-related mutations can trigger complex phenotypes depending on the affected gene and mutation.[1,4] To assess the phenotypic changes after HDR repair, we differentiated several hiPS cell lines into retinal cellular models. Notably, pathogenic variant correction and pluripotency conservation were routinely checked during hiPS culture and after differentiation (Figures S4A and S4B).

Bestrophin-1, encoded by *BEST1*, is an integral membrane protein that functions as a calcium-activated anion channel, and is expressed only in RPE cells.[24,72] Thus, we differentiated BEST1 FRIMOi006-A parental and knocked-in clones into this retinal cell type. Both genotypes exhibited normal RPE differentiation and morphology as revealed by ZO-1 staining, the expression of early differentiation markers (*PAX6* and *MITF*), and the RPE marker RPE65 (Figures 4A and S4C). We also evaluated the mRNA levels of *BEST1* and found similar expression in wild-type, parental, and corrected RPE cells (Figure 4B), demonstrating that this pathogenic variant does not significantly affect bestrophin-1 expression, as previously reported.[73]

Calcium-activated chloride channel activity was measured by quantifying iodide distribution in RPE cells expressing a fluorescent sensor (Figure S4D). Once the chloride channels are opened, iodide ions enter the cell—quenching fluorescence of the transfected RPE cells, revealing channel activation. We observed that the corrected FRIMOi006-A clones displayed reduced opening of the chloride channel over time compared with the parental clones and showed similar levels to those found in wild-type RPE (Figure 4C), even in the presence of an ionophore (Figure 4D). The fluorescence signal was lower in *BEST1* mutant cells at almost all time points analyzed compared with isogenic knockin clones (Figures 4C and 4D). In contrast, no differences were observed when the RPE cells were cultured without a stimulus buffer (Figure S4E). These results demonstrate restoration of the previously reported *BEST1* c.229C>T (p.Pro77Ser) phenotype, showing a reduction in chloride channel opening in CRISPR-Cas9-corrected cells and restoration of epithelial permeability.[73]

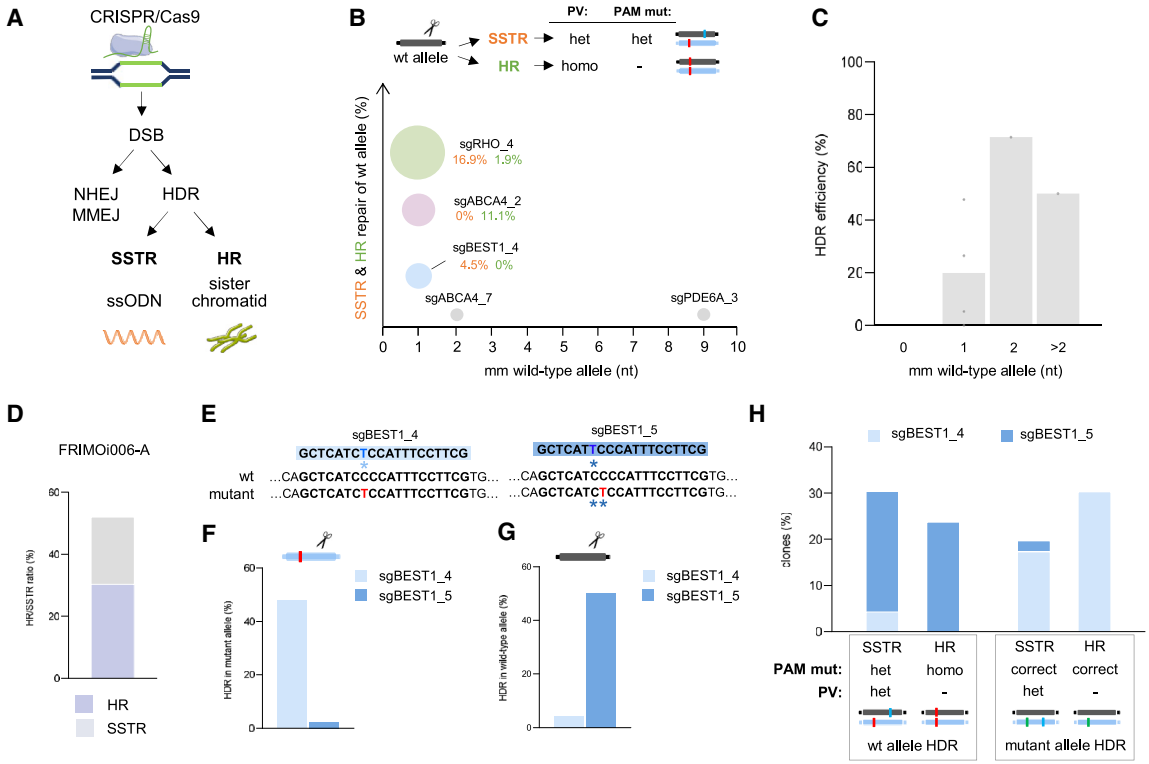

Figure 2. Precise HDR correction of pathogenic variants by using the endogenous sister chromatid

(A) DNA repair pathways used after CRISPR-Cas9-induced DSB. (B) Percentage of SSTR- and HR-correction in wild-type allele in assays of heterozygous carriers of Figure 1D. (C) Percentage of HDR-mediated correction of the pathogenic variant according to the number of mismatches in homology with the wild-type allele of the sgRNA used. (D) HR and SSTR ratio obtained in the gene-editing assay in FRIMOi006-A. (E) Scheme of sgBEST1_4 and sgBEST1_5 homologies against wild-type and mutant alleles in FRIMOi006-A. Asterisks indicate mismatch in the sequence homology. In red is shown the pathogenic variant and in blue the nucleotide change in the sgRNA. (F) Total HDR efficiency in editing the mutant allele in the assays with sgBEST1_4 or sgBEST1_5 in FRIMOi006-A. (G) As in (F) but in the wild-type allele. (H) HDR-mediated correction data obtained with sgBEST1_4 or sgBEST1_5 according to the pathogenic variant (in green corrected, in red not corrected) and PAM mutation (in blue) in FRIMOi006-A wild-type and mutant alleles.

Next, we investigated whether epithelial function was compromised in *BEST1* mutant RPE. RPE cells are essential for photoreceptor function by phagocytosing photoreceptor outer segments (POSs).[74,75] Notably, FRIMOi006-A parental cells displayed increased POS uptake compared with the corrected clones, indicating enhanced phagocytic activity of *BEST1* mutant cells (Figures 4E and S4F). Nevertheless, this increase in phagocytosis can hamper POS processing and accumulation in RPE cells causing abnormal function, which has been associated with visual affectations.[76] We also monitored *trans*-epithelial electrical resistance (TER) in RPE monolayers. Surprisingly, *BEST1* c.229C>T-repaired clones displayed increased TER compared with mutant cells (Figure 4F). This result suggests a role for the epithelial barrier function with bestrophin-1.

Collectively, these functional data reveal a potential rescue of the retinal phenotype associated with IRD-related mutations after gene editing. The disease-associated phenotype in Best disease was reversed by restoring the epithelial monolayer function and permeability.

DISCUSSION

Pathogenic variants associated with IRDs have been identified in more than 300 genes, and lead to diverse outcomes and cellular effects. This underscores the need for various therapeutic approaches to address these issues effectively. Most IRDs are caused by point mutations, such as those corrected by gene editing in this study, making technologies promising tools for future personalized medicine. In addition, genome editing has improved significantly in recent years with the advent of prime and base editors, and the enhancement of Cas enzymes and other engineered proteins, has considerably enhanced their potential.[24,77,78]

The data obtained in this study show the precise correction of IRD-related pathogenic variants using CRISPR-Cas9 and TALEN technologies. Gene-editing results showed that targeting homozygous mutations, point insertions, or deletions yielded the best HDR efficiencies, coinciding with the absence or lowest ratios of on-target defects (Figures 1E and 1F). In our study, CRISPR-Cas9 was found to be significantly more powerful than TALENs, demonstrating higher sgRNA-induced DSB and HDR efficiency in hiPSCs. In the majority of assays,

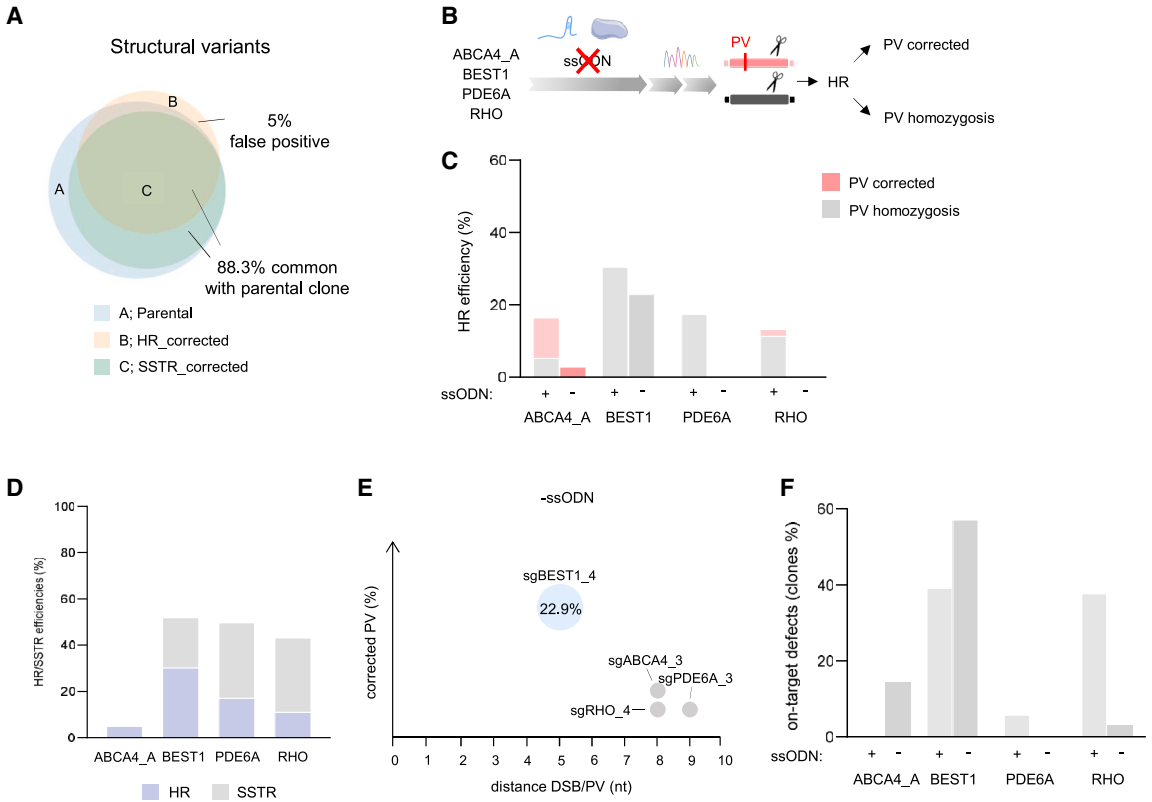

Figure 3. Pathogenic variant correction by using the wild-type allele as repair template in ssODN-free CRISPR-Cas9 gene-editing assay

(A) Venn diagram showing structural variants results found in long-read sequencing in FRIMOi006-A clones. (B) Schematic of the gene-editing assay performed without transfecting the ssODN. (C) Percentage of HR-corrected clones obtained in the assays performed with or without ssODN. (D) Gene-editing ratios based on SSTR or HR repair mechanisms in each hiPS cell line. (E) Representation of percentage of clones with the pathogenic variant corrected in the assays performed without the ssODN depending on the distance between the DSB and the pathogenic variant. (F) Quantification of on-target defects in each assay.

we successfully corrected more than 45% of the screened clones. However, although less effective, TALENs could be useful and suitable in cases where CRISPR-Cas9 is not, due to genomic loci concerns. Similarly, engineered Cas enzymes—like, Cas12a, Cas13, and Cas14—have been shown promoting CRISPR-Cas applications.[53,77–79]

The efficiency of inducing DNA cleavage by sgRNA is a key factor in the design of CRISPR assays.[53,80,81] Nevertheless, the optimization of other aspects could also significantly improve gene-editing outcomes. For instance, the number of mismatches in sequence homology determines allele discrimination by sgRNA, which results in an advantage in point mutations affecting two or more nucleotides because the wild-type allele is virtually unrecognized. The results reported here show that sgRNA specificity is of utmost importance for preventing undesired genomic events in the wild-type allele. In addition, the distance between the DSB and the pathogenic variant is decisive for proper gene editing, as previously reported.[66,68]

DNA lesions are preferably resolved by the NHEJ pathway in somatic mammalian cells.[40,71] Therefore, in gene-editing assays, the HDR mechanism is commonly favored through the use of HDR activators and NHEJ inhibitors.[82] Recent studies correlate the importance of the chromatin status in the regulation of the DSB repair mechanism used and also in the sgRNA-mediated ability to cleave DNA.[83,84] Surprisingly, in the assays for correcting heterozygous pathogenic variants we observed a significant amount of corrected clones that had not incorporated the Cas9-blocking mutation—present in the ssODN—and a small percentage of edited clones carrying the pathogenic variant in homozygosis. These results suggest DNA repair methods other than ssODN-mediated correction. Recombinases like RAD51/RAD52 have been reported to be key mediators of Cas9-induced DSB with a dependence on the type of repair template.[45,85] For instance, RAD52 promotes single-stranded DNA increasing SSTR pathway.[86] Notably, preliminary data in this study showed a potential association in *RAD52* expression levels and SSTR-mediated repair (data not shown).

Noteworthy, the DNA DSB could be resolved using the ssODN but failing to incorporate the Cas9-blocking mutation because of template unbinding or instability. Additionally, a large DNA deletion in the wild-type allele may explain the fictitious detection of the pathogenic variants in homozygosis. However, karyotyping analysis and long-read sequencing revealed the absence of structural variants or gross

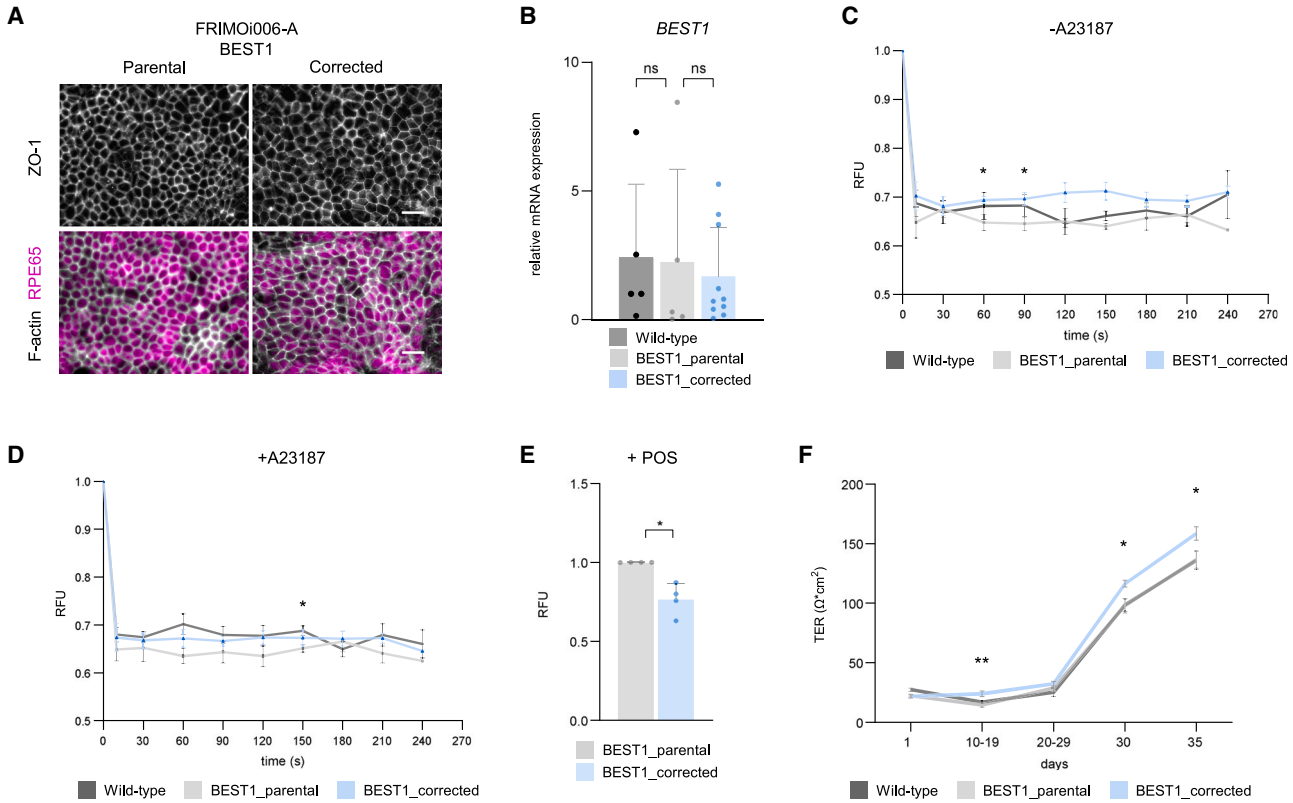

Figure 4. HDR-corrected clones exhibit reversion of the mutant-associated phenotype in retinal cellular models

(A) Immunofluorescence staining of ZO-1 or F-actin and RPE65 markers in differentiated RPE FRIMOi006-A clones. Scale bar represents 25 μm. (B) Relative mRNA expression of *BEST1* in RPE cells of wild-type and FRIMOi006-A clones. (C) Relative fluorescence quantification of the YFP-labeled Premo Halide Sensor recorded every 30 s for 2 min with the stimulus buffer in RPE cells derived from wild-type, parental, and corrected (SSTR and HR) FRIMOi006-A clones. Data are the average of four independent experiments with different clones of each genotype and represented as mean ± SEM. (D) As in (C) but in the presence of the ionophore A23187. (E) Relative fluorescence units in RPE cultures of parental and corrected FRIMOi006-A clones in the presence of FITC-labeled POS. Data are the average of four independent experiments. (F) *Trans*-epithelial electrical resistance recordings in wild-type and FRIMOi006-A RPE during cell culture in transwells. Data represent mean ± SEM. $p \leq 0.001$ (***), $p \leq 0.01$ (**), $p \leq 0.05$ (*) levels, or non-significant (ns) for $p > 0.05$.

deletions, which could lead to misidentification of clones. Moreover, these genomic events are often associated with the plasmidic delivery of sgRNA/Cas9 rather than with ribonucleoprotein (RNP) complexes.[87–89] Noteworthy, despite being potentially deleterious, these undesired homozygous clones can still be edited in subsequent rounds of gene editing.

Notably, DSB repair using endogenous homologous DNA was further supported by performing a CRISPR-Cas9 assay by transfecting only sgRNA and Cas9 but not ssODN. This assay successfully corrected the heterozygous pathogenic variant of *BEST1*. However, this was not achieved in ABCA4_A, PDE6A, and RHO hiPSCs, suggesting that successful DSB repair by the HR pathway could be intimately ligated to the gene, mutation, and hiPS cell line per se. Accordingly, the HR and SSTR pathways are regulated by several proteins that can be influenced by these factors.[34,49]

Remarkably, several studies have reported successful template-free repair of DSB through the NHEJ/MMEJ pathways, which are sufficient to recover protein function.[90–92] Nevertheless, this approximation is not suitable for the precise correction of single-nucleotide pathogenic variants. Similarly, the MMEJ pathway has been reported to be useful for correcting small indel variants via stochastic repair.[93]

Altogether, these findings suggest the possibility of using CRISPR-Cas9 gene editing without transfecting a synthetic oligonucleotide for the precise correction of pathogenic variants. Consequently, the transfection cargo is reduced, and the potential on- and off-target effects associated with the ssODN.[53,66] Noteworthy, this approximation lacks the modification in the PAM sequence, which could result in an increase in NHEJ events due to DNA re-cut.

Gene editing as a therapeutic strategy needs to ultimately reverse the disease condition of the patient to stop the mutant phenotype. Importantly, we observed rescue of anionic intracellular transport in *BEST1* c.229C>T corrected clones, which was reported to be increased in mutant *BEST1* RPE cells compared with wild-type cells (Figures 4C and 4D).[94] We also found increased permeability of the *BEST1*

mutant RPE monolayer compared with that in repaired cells in TER measurements (Figure 4F). The electrical resistance of the epithelial layer is directly associated with monolayer permeability. Thus, the higher ion flux across mutant RPE cells and their increased phagocytic activity suggest a reduced tightness of the epithelial barrier in bestrophin-1-mutant cells, which could lead to RPE dysfunction.

In summary, we report the efficient correction of different iPS cell lines derived from patients with several IRDs (Stargardt disease, Best disease, achromatopsia, and retinitis pigmentosa). We achieved a highly efficient CRISPR-Cas9-mediated correction of a homozygous mutation in *PDE6C* and of small ins/del in *ABCA4* and *PDE6A*, respectively. Additionally, we report the successful TALEN-mediated correction of the FRIMOi002-A *USH2A* mutant cell line. Furthermore, gene-editing results suggest the potential use of CRISPR-Cas9 without the use of ssODNs as exogenous repair templates and DSB resolution using endogenous DNA, which could be suitable for personalized medicine. Finally, the HDR-repaired clones exhibited the restoration of several mutant-associated conditions.

Considerable efforts are being made to find therapeutic approximations to cure the majority of IRDs, especially in gene therapy, antisense oligonucleotides, optogenetics, and stem cell-based therapies.[95–98] Gene therapy is one of the most explored modalities for treating these retinal disorders. Nevertheless, in some cases, it could be challenging because of several issues such as transgene size, inflammation, dosage, and use of appropriate vectors.[99–101] Although gene editing also shares some of the concerns that need to be addressed by gene replacement, this editing therapy allows permanent correction of the patient's own DNA, stopping disease progression.

Notably, patient-derived hiPSCs in combination with gene editing represent a significant stem cell-based strategy for IRD management, considering that knocked-in clones display the rescue of the potential disease-associated phenotype triggered by the pathogenic variant. Moreover, recent studies have shown encouraging short-term results on the safety and survival of transplanted hiPSC-derived RPE cells in animal and human models.[21,102,103]

One of the remaining steps should be to enhance gene-editing studies in retinal tissues, taking into consideration several key factors such as delivery, safety, and transfection methodologies. The eye is a relatively accessible organ, which confers an advantage for therapy development. Research on gene and cell therapy is critical for the regenerative and personalized medicine. Altogether these data contribute to improving the study and development of potential therapeutic approaches to stop disease progression and encourage the advancement of gene-editing strategies for the future cure of IRD.

MATERIALS AND METHODS

Human iPSC culture and lineage differentiation

Human iPS cell lines FRIMOi001-A, 002-A, 003-A, 004-A, 005-A, 006-A, and 007-A, described in Table 1, were obtained as previously described.[61,62,64,65,104,105] For some experiments, wild-type hiPSCs were used from a patient without any ophthalmologic disease and no genetic variants related to retinal dystrophies. hiPSC colonies were maintained in StemFlex medium (Thermo Fisher Scientific, Waltham, MA, USA) and cultured on Matrigel-coated dishes (Merck, Bedford, MA, USA). To obtain hiPS single-cell suspensions, hiPS colonies were detached using TrypLE (Thermo Fisher Scientific), centrifuged, and counted before Neon-mediated transfection (Thermo Fisher Scientific). For hiPSC lineage specification, gene-edited clones were subjected to ectodermal, mesodermal, and endodermal differentiation using the Human Pluripotent Stem Cell Functional Identification Kit (R&D Systems, Minneapolis, MN, USA), according to the manufacturer's instructions. The study was conducted in accordance with the Declaration of Helsinki and was approved by the Ethics Committee of the Institut de Microcirurgia Ocular (Protocol code: 170505_117. Date of approval: June 2, 2017).

sgRNAs, TALENs, and ssODNs design

sgRNAs and TALENs were designed using the Invitrogen TrueDesign Genome Editor (Thermo Fisher Scientific) and are listed in Table S1. ssODNs were designed of 70–86 nucleotides total length and synthesized using PAGE purification method. The pathogenic variant was located at the center of the template, with the left and right arms at 30–35 nucleotides perfectly homologous to the target sequence. Phosphorothioate nucleotide modifications were added to the ends of ssODNs to increase their stability. The ssODN for the CRISPR assays also harbored a Cas9-blocking mutation to modify the PAM sequence, which was analyzed using ALAMUT software (version 1.4, Sophia Genetics), PhyloP, and the UCSC Genome Browser for the conservation of the reading frame, amino acid change, and SNP prevalence.

Genomic cleavage detection assay

The efficiency of DNA cleavage induced by sgRNAs and TALENs was determined using GeneArt Genomic Cleavage Detection kit (Thermo Fisher Scientific) according to the manufacturer's instructions. Briefly, hiPSCs were transfected with sgRNA or TALEN and 4 days later, PCR amplification of the desired locus was performed. A single band was confirmed by agarose gel electrophoresis. Next, the PCR product was subjected to several rounds of denaturation and re-annealing to generate mismatches that were detected and cleaved by the Detection Enzyme. The resulting bands were visualized by agarose gel electrophoresis using iBrightCL1000 (Thermo Fisher Scientific). Quantification of band intensity for correlation with Cas9 activity was performed using iBright Analysis Software (Thermo Fisher Scientific).

Gene-editing assay

For gene editing, 1×10^5 hiPSCs were electroporated (Neon, Thermo Fisher Scientific) with two pulses of 20 ms at 1,200 V for transfection with 10 pmol sgRNA, 15 pmol ssODN, and 10 pmol High Fidelity (HiFi) SpCas9 protein (Thermo Fisher Scientific). Simultaneously, hiPSCs without sgRNA and ssODN were transfected as parental controls. Immediately after electroporation, hiPSCs were seeded onto Matrigel-coated dishes and cultured in StemFlex medium supplemented

with 10 μM ROCK inhibitor (Merck, Bedford, MA, USA), 10 μM of the HDR activator L755507 (Merck), and 0.5 μM of NHEJ inhibitor M3814 (Selleckchem, Houston, TX, USA) for 24 h. Then, cell culture medium was replaced with fresh StemFlex medium, and cells were cultured until formation of single colonies. When colonies grew but were still small enough to ensure the formation of individual clones, they were picked and cultured individually in 96-multiwell plates. After approximately 1 week, the clones were expanded, and a fraction of the cells from each clone was collected for genotyping analysis by Sanger sequencing (Macrogen, Madrid, Spain). The parental and properly edited clones were expanded and sequenced to confirm their genotypes. Notably, the edited clones in each assay were analyzed for other rare variants or patient-specific SNPs to ensure cell line purity.

PCR amplification, Sanger sequencing, and karyotyping

PCR amplification of the desired genomic region was performed and run on a gel to ensure a single DNA band and a negative control. The PCR products were purified using 96-well Acroprep Advance plates (Pall Corporation, Ann Arbor, MI, USA) with a vacuum manifold (Pall Corporation). The products were Sanger sequenced using forward and reverse primers (Macrogen). All primer sequences used in this study are listed in Tables S6 and S7. Sanger sequencing results were downloaded from the manufacturer's platform and the data were aligned and analyzed. Gene-edited clones were also analyzed for the presence of other uncommon variants to confirm hiPS cell line purity. Parental and edited clones were subjected to karyotyping (Reference Laboratory, Spain).

Off-target prediction and analysis

Off-target prediction was performed using the online tool Cas-OFFinder.[106] Up to three mismatches were allowed for the algorithm to perform the prediction. All exonic and intronic regions in close proximity to the exons were covered by Sanger sequencing. In addition, potential splicing effects in deep intronic off-targets were predicted using the ALAMUT software (Sophia Genetics). Intergenic regions were not analyzed in this study. PCR amplification and Sanger sequencing of selected off-targets (Table S7) were performed on the parental and corrected clones.

Nanopore sequencing

Long-read sequencing was performed using Oxford Nanopore sequencing (LongSeq Applications, Spain). Briefly, DNA was extracted from cells using Gentra Puregene Cell Kit (Qiagen, Netherlands) and analyzed for purity and quality. Data were aligned via the Minimap2-specific algorithm for Oxford Nanopore Genomic Reads and QualiMap. Structural variant calling was performed with Sniffles and annotated with SnpEff and SnpSift, according to the LongSeq report. Structural variants with at least 30 reads were used for data interpretation.

hiPSCs differentiation into retinal cellular models

hiPSCs were differentiated into retinal organoids, RPEs, and photoreceptor-like cells as described by de Bruijn et al., Gonzalez-Cordero et al.,[107,108] Regent et al.,[73] and Barnea-Cramer et al.,[109] respectively. Briefly, for organoids differentiation, hiPSCs were cultured in proneural induction media, and optic vesicles were excised and cultured in low-binding 96-multiwell plates in several retinal differentiation mediums until maturation. RPEs were obtained either by the same retinal organoids protocol or by culturing hiPSCs in RPE differentiation media subsequently supplemented with 10 mM Nicotinamide (Sigma), 100 ng/mL Activin A (Stem Cell Technologies), or 3 μM CHIR99021 (Sigma). RPE cell pigmentation was evaluated using ImageJ software (NIH, Bethesda, MD, USA).

Immunofluorescence staining

For immunofluorescence analysis of RPE differentiation markers, iPSC clones were seeded and differentiated at the desired time points onto Matrigel-coated ibidi slides (ibidi GmbH, Gräfeling, Germany). ibidi slides were fixed in 4% paraformaldehyde (Thermo Fisher Scientific) for 15 min at room temperature. Next, the cells were permeabilized with 0.25% Triton X-100 in phosphate-buffered saline (PBS) and incubated for 1 h in blocking solution (5% fetal bovine serum, 4% bovine serum albumin, and 0.5% Tween in PBS) at room temperature. Fixed parental and edited clones were incubated overnight at 4°C with ZO-1 (ZO1-1A12, Thermo Fisher Scientific), RPE65 (401.8B11.3D9, Thermo Fisher Scientific) or Alexa Fluor Plus 555 phalloidin (A30106, Thermo Fisher Scientific). The cells were visualized using an anti-mouse Alexa Fluor 488 (A32723, Thermo Fisher Scientific) secondary antibody and counterstained with 4′,6-diamidino-2-phenylindole (DAPI) (62248, Thermo Fisher Scientific). Immunofluorescence imaging was performed using Zeiss Axiovert and Axiocam 503 mono (Carl Zeiss Inc., Jena, Germany), and images were processed using ImageJ software (NIH). Representative images are shown.

RNA extraction and quantitative real-time PCR

To assess the gene expression of pluripotency and RPE differentiation markers, RNA was extracted using TRIzol reagent (Thermo Fisher Scientific) according to the manufacturer's instructions. cDNA was obtained using Transcriptor First Strand cDNA Synthesis Kit (Roche Diagnostics, Basel, Switzerland) and analyzed by real-time PCR using QuantStudio and specific TaqMan probes (Thermo Fisher Scientific).

TER measurement

For electrical resistance assessment, 1×10^5 RPE cells were seeded onto Matrigel-coated Transwell filters (0.4-μm pore size, 0.47-cm^2 area, Thermo Fisher Scientific), and cultured in RPE media. Medium was also added to the lower compartment. TER was recorded during monolayer maturation and in Transwell filters without cells for background subtraction once per week for more than 1 month using a voltohmmeter (Millicell ERS 3.0 digital, Merck). TER measurements were obtained by multiplying the net TER values by the culture area.

POS isolation, labeling, and phagocytosis by RPE

POSs were isolated from porcine eyes according to the protocol described by Parinot et al.[110] Once purified, POSs were observed under a microscope to assess their morphology. One portion was labeled with fluorescein isothiocyanate (FITC), and then were aliquoted and

frozen for storage. RPE cultures of parental and edited FRIMOi006-A clones were seeded in 96-multiwell plates, and mature RPE cells were incubated with 1×10^6 FITC-labeled POSs for 8 h. The POS-containing medium was removed, and the RPE cells were washed five times with PBS. Wells without cells were used as controls to ensure POS removal, and cells without POS were used for background subtraction. FITC fluorescence was determined using Varioskan LUX (Thermo Fisher Scientific).

Anion channel activity determination

The influx across chloride channels was quantified using the Premo Halide Sensor kit (Thermo Fisher Scientific) following the manufacturer's instructions. Briefly, RPE cells were seeded in 96-multiwell plates and transduced with a YFP-labeled sensor for halide ions. Anion channel activity was stimulated with a buffer containing NaI supplemented or not with A23187 (10 μg/mL). The fluorescence signal was quenched when the chloride channel was activated. Fluorescence was detected every 30 s using Varioskan LUX (Thermo Fisher Scientific) and background well values were subtracted from the experimental wells.

Statistical analysis

Statistical analyses were performed using the Prism 9.3.1 (GraphPad Software, La Jolla, CA, USA). Statistical significance was assessed using the non-parametric Mann-Whitney *U* test and set at values of $p \leq 0.001$ (***), $p \leq 0.01$ (**), $p \leq 0.05$ (*) levels, or non-significant (ns) for $p > 0.05$. Bar graphs represent mean ± SD, unless specified. In each experiment at least two clones of each genotype were used for analysis. Both SSTR- and HR-corrected clones were used for functional data production in Figure 4.

DATA AVAILABILITY

The authors declare that all relevant data supporting the findings of this study are available within the article and its supplemental information. Raw data and additional not shown results are available from the corresponding author (E.P.) upon reasonable request.

ACKNOWLEDGMENTS

We are grateful to Sheila Ruiz-Nogales for her technical support and helpful comments on the manuscript. We are also indebted to the patients for their contributions to the study. Informed consent was obtained from the subjects involved in the study. This work was supported by grant number Fi-201401 (Fundació de Recerca de l'Institut de Microcirurgia Ocular, Fundación IMO). The authors also thank Bernard Faure for his contribution.

AUTHOR CONTRIBUTIONS

L.S. performed the experimental work and analysis in the study; L.S. and E.P. contributed to project conceptualization and methodology; E.P. conceived and supervised the study; L.S. wrote the manuscript; and E.P. supervised the manuscript.

DECLARATION OF INTERESTS

The authors declare no conflict of interest.

SUPPLEMENTAL INFORMATION

Supplemental information can be found online at https://doi.org/10.1016/j.omtn.2025.102482.

REFERENCES

1. Tatour, Y., and Ben-Yosef, T. (2020). Syndromic inherited retinal diseases: genetic, clinical and diagnostic aspects. Diagnostics *10*, 779. https://doi.org/10.3390/diagnostics10100779.

2. Mansfield, B.C., Yerxa, B.R., and Branham, K.H. (2020). Implementation of a registry and open access genetic testing program for inherited retinal diseases within a non-profit foundation. Am. J. Med. Genet. C Semin. Med. Genet. *184*, 838–845. https://doi.org/10.1002/ajmg.c.31825.

3. Hanany, M., Rivolta, C., and Sharon, D. (2020). Worldwide carrier frequency and genetic prevalence of autosomal recessive inherited retinal diseases. Proc. Natl. Acad. Sci. USA *117*, 2710–2716. https://doi.org/10.1073/pnas.1913179117.

4. Schneider, N., Sundaresan, Y., Gopalakrishnan, P., Beryozkin, A., Hanany, M., Levanon, E.Y., Banin, E., Ben-Aroya, S., and Sharon, D. (2022). Inherited retinal diseases: Linking genes, disease-causing variants, and relevant therapeutic modalities. Prog. Retin. Eye Res. *89*, 101029. https://doi.org/10.1016/j.preteyeres.2021.101029.

5. Biswas, P., Villanueva, A.L., Soto-Hermida, A., Duncan, J.L., Matsui, H., Borooah, S., Kurmanov, B., Richard, G., Khan, S.Y., Branham, K., et al. (2021). Deciphering the genetic architecture and ethnographic distribution of IRD in three ethnic populations by whole genome sequence analysis. PLoS Genet. *17*, e1009848. https://doi.org/10.1371/journal.pgen.1009848.

6. Daich Varela, M., Bellingham, J., Motta, F., Jurkute, N., Ellingford, J.M., Quinodoz, M., Oprych, K., Niblock, M., Janeschitz-Kriegl, L., Kaminska, K., et al. (2023). Multidisciplinary team directed analysis of whole genome sequencing reveals pathogenic non-coding variants in molecularly undiagnosed inherited retinal dystrophies. Hum. Mol. Genet. *32*, 595–607. https://doi.org/10.1093/hmg/ddac227.

7. Fenner, B.J., Tan, T.E., Barathi, A.V., Tun, S.B.B., Yeo, S.W., Tsai, A.S.H., Lee, S.Y., Cheung, C.M.G., Chan, C.M., Mehta, J.S., and Teo, K.Y.C. (2022). Gene-Based Therapeutics for Inherited Retinal Diseases. Front. Genet. *12*, 794805. https://doi.org/10.3389/fgene.2021.794805.

8. Song, D.J., Bao, X.L., Fan, B., and Li, G.Y. (2023). Mechanism of Cone Degeneration in Retinitis Pigmentosa. Cell. Mol. Neurobiol. *43*, 1037–1048. https://doi.org/10.1007/s10571-022-01243-2.

9. Tsang, S.H., and Sharma, T. (2018). Stargardt Disease. Adv. Exp. Med. Biol. *1085*, 139–151. https://doi.org/10.1007/978-3-319-95046-4_27.

10. Brunetti-Pierri, R., Karali, M., Melillo, P., Di Iorio, V., De Benedictis, A., Iaccarino, G., Testa, F., Banfi, S., and Simonelli, F. (2021). Clinical and molecular characterization of achromatopsia patients: A longitudinal study. Int. J. Mol. Sci. *22*, 1681. https://doi.org/10.3390/ijms22041681.

11. Maguire, A.M., Bennett, J., Aleman, E.M., Leroy, B.P., and Aleman, T.S. (2021). Clinical Perspective: Treating RPE65-Associated Retinal Dystrophy. Mol. Ther. *29*, 442–463. https://doi.org/10.1016/j.ymthe.2020.11.029.

12. Kang, C., and Scott, L.J. (2020). Voretigene Neparvovec: A Review in RPE65 Mutation-Associated Inherited Retinal Dystrophy. Mol. Diagn. Ther. *24*, 487–495. https://doi.org/10.1007/s40291-020-00475-6.

13. Fischer, M.D., Michalakis, S., Wilhelm, B., Zobor, D., Muehlfriedel, R., Kohl, S., Weisschuh, N., Ochakovski, G.A., Klein, R., Schoen, C., et al. (2020). Safety and Vision Outcomes of Subretinal Gene Therapy Targeting Cone Photoreceptors in Achromatopsia: A Nonrandomized Controlled Trial. JAMA Ophthalmol. *138*, 643–651. https://doi.org/10.1001/jamaophthalmol.2020.1032.

14. Michalakis, S., Gerhardt, M., Rudolph, G., Priglinger, S., and Priglinger, C. (2022). Achromatopsia: Genetics and Gene Therapy. Mol. Diagn. Ther. *26*, 51–59. https://doi.org/10.1007/s40291-021-00565-z.

15. Trapani, I. (2018). Dual AAV vectors for stargardt disease. In Methods in Molecular Biology. https://doi.org/10.1007/978-1-4939-7522-8_11.

16. Lu, Y., Godbout, K., Lamothe, G., and Tremblay, J.P. (2023). CRISPR-Cas9 delivery strategies with engineered extracellular vesicles. Mol. Ther. Nucleic Acids *34*, 102040. https://doi.org/10.1016/j.omtn.2023.102040.

17. Cremers, F.P.M., Lee, W., Collin, R.W.J., and Allikmets, R. (2020). Clinical spectrum, genetic complexity and therapeutic approaches for retinal disease caused by ABCA4 mutations. Prog. Retin. Eye Res. *79*, 100861. https://doi.org/10.1016/j.preteyeres.2020.100861.

18. Francia, S., Shmal, D., Di Marco, S., Chiaravalli, G., Maya-Vetencourt, J.F., Mantero, G., Michetti, C., Cupini, S., Manfredi, G., DiFrancesco, M.L., et al. (2022). Light-induced charge generation in polymeric nanoparticles restores vision in advanced-stage retinitis pigmentosa rats. Nat. Commun. *13*, 3677. https://doi.org/10.1038/s41467-022-31368-3.

19. Sun, D., Schur, R.M., Sears, A.E., Gao, S.Q., Vaidya, A., Sun, W., Maeda, A., Kern, T., Palczewski, K., and Lu, Z.R. (2020). Non-viral Gene Therapy for Stargardt Disease with ECO/pRHO-ABCA4 Self-Assembled Nanoparticles. Mol. Ther. *28*, 293–303. https://doi.org/10.1016/j.ymthe.2019.09.010.

20. Yamanaka, S. (2020). Pluripotent Stem Cell-Based Cell Therapy—Promise and Challenges. Sci. Transl. Med. *4*, 127ps9. https://doi.org/10.1016/j.stem.2020.09.014.

21. Klymenko, V., González Martínez, O.G., and Zarbin, M. (2024). Recent Progress in Retinal Pigment Epithelium Cell-Based Therapy for Retinal Disease. Stem Cells Transl. Med. *13*, 317–331. https://doi.org/10.1093/stcltm/szae004.

22. Pulman, J., Sahel, J.A., and Dalkara, D. (2022). New Editing Tools for Gene Therapy in Inherited Retinal Dystrophies. CRISPR J. *5*, 377–388. https://doi.org/10.1089/crispr.2021.0141.

23. Li, H., Yang, Y., Hong, W., Huang, M., Wu, M., and Zhao, X. (2020). Applications of genome editing technology in the targeted therapy of human diseases: mechanisms, advances and prospects. Signal Transduct. Targeted Ther. *5*, 1. https://doi.org/10.1038/s41392-019-0089-y.

24. van der Oost, J., and Patinios, C. (2023). The genome editing revolution. Trends Biotechnol. *41*, 396–409. https://doi.org/10.1016/j.tibtech.2022.12.022.

25. Sharma, G., Sharma, A.R., Bhattacharya, M., Lee, S.S., and Chakraborty, C. (2021). CRISPR-Cas9: A Preclinical and Clinical Perspective for the Treatment of Human Diseases. Mol Ther. *29*, 571–586. https://doi.org/10.1016/j.ymthe.2020.09.028.

26. Khan, S.H. (2019). Genome-Editing Technologies: Concept, Pros, and Cons of Various Genome-Editing Techniques and Bioethical Concerns for Clinical Application. Mol. Ther. Nucleic Acids *16*, 326–334. https://doi.org/10.1016/j.omtn.2019.02.027.

27. Maeder, M.L., Stefanidakis, M., Wilson, C.J., Baral, R., Barrera, L.A., Bounoutas, G.S., Bumcrot, D., Chao, H., Ciulla, D.M., DaSilva, J.A., et al. (2019). Development of a gene-editing approach to restore vision loss in Leber congenital amaurosis type 10. Nat. Med. *25*, 229–233. https://doi.org/10.1038/s41591-018-0327-9.

28. Pierce, E.A., Aleman, T.S., Ashimatey, B., Kim, K., Rashid, R., Myers, R., and Pennesi, M.E. (2023). Safety and Efficacy of EDIT-101 for Treatment of CEP290-associated Retinal Degeneration. Investigative Ophthalmology & Visual Science *64*, 3785.

29. Feng, Y., Sassi, S., Shen, J.K., Yang, X., Gao, Y., Osaka, E., Zhang, J., Yang, S., Yang, C., Mankin, H.J., et al. (2015). Targeting Cdk11 in osteosarcoma cells using the CRISPR-cas9 system. J. Orthop. Res. *33*, 199–207. https://doi.org/10.1002/jor.22745.

30. Tang, H., and Shrager, J.B. (2016). CRISPR/Cas-mediated genome editing to treat EGFR -mutant lung cancer: a personalized molecular surgical therapy. EMBO Mol. Med. *8*, 83–85. https://doi.org/10.15252/emmm.201506006.

31. Valletta, S., Dolatshad, H., Bartenstein, M., Yip, B.H., Bello, E., Gordon, S., Yu, Y., Shaw, J., Roy, S., Scifo, L., et al. (2015). ASXL1 mutation correction by CRISPR/Cas9 restores gene function in leukemia cells and increases survival in mouse xenografts. Oncotarget *6*, 44061–44071. https://doi.org/10.18632/oncotarget.6392.

32. Long, C., McAnally, J.R., Shelton, J.M., Mireault, A.A., Bassel-Duby, R., and Olson, E.N. (2014). Prevention of muscular dystrophy in mice by CRISPR/Cas9-mediated editing of germline DNA. Science *345*, 1184–1188. https://doi.org/10.1126/science.1254445.

33. Ebina, H., Misawa, N., Kanemura, Y., and Koyanagi, Y. (2013). Harnessing the CRISPR/Cas9 system to disrupt latent HIV-1 provirus. Sci. Rep. *3*, 2510. https://doi.org/10.1038/srep02510.

34. Chen, J., Sathiyamoorthy, K., Zhang, X., Schaller, S., Perez White, B.E., Jardetzky, T.S., and Longnecker, R. (2018). Ephrin receptor A2 is a functional entry receptor for Epstein-Barr virus. Nat. Microbiol. *3*, 172–180. https://doi.org/10.1038/s41564-017-0081-7.

35. Yoshiba, T., Saga, Y., Urabe, M., Uchibori, R., Matsubara, S., Fujiwara, H., and Mizukami, H. (2019). CRISPR/Cas9-mediated cervical cancer treatment targeting human papillomavirus E6. Oncol. Lett. *17*, 2197–2206. https://doi.org/10.3892/ol.2018.9815.

36. Becker, S., and Boch, J. (2021). TALE and TALEN genome editing technologies. Gene Genome *2*, 100007. https://doi.org/10.1016/j.ggedit.2021.100007.

37. Shamshirgaran, Y., Liu, J., Sumer, H., Verma, P.J., and Taheri-Ghahfarokhi, A. (2022). Tools for Efficient Genome Editing; ZFN, TALEN, and CRISPR. Methods Mol. Biol. *2495*, 29–46. https://doi.org/10.1007/978-1-0716-2301-5_2.

38. Jain, S., Shukla, S., Yang, C., Zhang, M., Fatma, Z., Lingamaneni, M., Abesteh, S., Lane, S.T., Xiong, X., Wang, Y., et al. (2021). TALEN outperforms Cas9 in editing heterochromatin target sites. Nat. Commun. *12*, 606. https://doi.org/10.1038/s41467-020-20672-5.

39. Lander, E.S. (2016). The Heroes of CRISPR. Cell *164*, 18–28. https://doi.org/10.1016/j.cell.2015.12.041.

40. Sander, J.D., and Joung, J.K. (2014). CRISPR-Cas systems for editing, regulating and targeting genomes. Nat. Biotechnol. *32*, 347–355. https://doi.org/10.1038/nbt.2842.

41. Wang, J.Y., and Doudna, J.A. (2023). CRISPR technology: A decade of genome editing is only the beginning. Science *379*, eadd8643. https://doi.org/10.1126/science.add8643.

42. Fu, Y.W., Dai, X.Y., Wang, W.T., Yang, Z.X., Zhao, J.J., Zhang, J.P., Wen, W., Zhang, F., Oberg, K.C., Zhang, L., et al. (2021). Dynamics and competition of CRISPR-Cas9 ribonucleoproteins and AAV donor-mediated NHEJ, MMEJ and HDR editing. Nucleic Acids Res. *49*, 969–985. https://doi.org/10.1093/nar/gkaa1251.

43. Ceccaldi, R., Rondinelli, B., and D'Andrea, A.D. (2016). Repair Pathway Choices and Consequences at the Double-Strand Break. Trends Cell Biol. *26*, 52–64. https://doi.org/10.1016/j.tcb.2015.07.009.

44. Yang, H., Ren, S., Yu, S., Pan, H., Li, T., Ge, S., Zhang, J., and Xia, N. (2020). Methods favoring homology-directed repair choice in response to crispr/cas9 induced-double strand breaks. Int. J. Mol. Sci. *21*, 6461. https://doi.org/10.3390/ijms21186461.

45. Richardson, C., Kelsh, R.N., and Richardson, R.J. (2023). New advances in CRISPR/Cas-mediated precise gene-editing techniques. Disease Models & Mechanisms *16*, dmm049874. https://doi.org/10.1242/dmm.049874.

46. Nambiar, T.S., Baudrier, L., Billon, P., and Ciccia, A. (2022). CRISPR-based genome editing through the lens of DNA repair. Mol. Cell *82*, 348–388. https://doi.org/10.1016/j.molcel.2021.12.026.

47. Bothmer, A., Phadke, T., Barrera, L.A., Margulies, C.M., Lee, C.S., Buquicchio, F., Moss, S., Abdulkerim, H.S., Selleck, W., Jayaram, H., et al. (2017). Characterization of the interplay between DNA repair and CRISPR/Cas9-induced DNA lesions at an endogenous locus. Nat. Commun. *8*, 13905. https://doi.org/10.1038/ncomms13905.

48. Jasin, M., and Haber, J.E. (2016). The democratization of gene editing: Insights from site-specific cleavage and double-strand break repair. DNA Repair *44*, 6–16. https://doi.org/10.1016/j.dnarep.2016.05.001.

49. Paulsen, B.S., Mandal, P.K., Frock, R.L., Boyraz, B., Yadav, R., Upadhyayula, S., Gutierrez-Martinez, P., Ebina, W., Fasth, A., Kirchhausen, T., et al. (2017). Ectopic expression of RAD52 and dn53BP1 improves homology-directed repair during CRISPR-Cas9 genome editing. Nat. Biomed. Eng. *1*, 878–888. https://doi.org/10.1038/s41551-017-0145-2.

50. Nami, F., Basiri, M., Satarian, L., Curtiss, C., Baharvand, H., and Verfaillie, C. (2018). Strategies for In Vivo Genome Editing in Nondividing Cells. Trends Biotechnol. *36*, 770–786. https://doi.org/10.1016/j.tibtech.2018.03.004.

51. Devkota, S. (2018). The road less traveled: Strategies to enhance the frequency of homology-directed repair (HDR) for increased efficiency of CRISPR/Cas-mediated transgenesis. BMB Rep. *51*, 437–443. https://doi.org/10.5483/BMBRep.2018.51.9.187.

52. Song, B., Yang, S., Hwang, G.H., Yu, J., and Bae, S. (2021). Analysis of nhej-based dna repair after crispr-mediated dna cleavage. Int. J. Mol. Sci. *22*, 6397. https://doi.org/10.3390/ijms22126397.

53. Schubert, M.S., Thommandru, B., Woodley, J., Turk, R., Yan, S., Kurgan, G., McNeill, M.S., and Rettig, G.R. (2021). Optimized design parameters for CRISPR Cas9 and Cas12a homology-directed repair. Sci. Rep. *11*, 19482. https://doi.org/10.1038/s41598-021-98965-y.

54. Rees, H.A., and Liu, D.R. (2018). Base editing: precision chemistry on the genome and transcriptome of living cells. Nat. Rev. Genet. *19*, 770–788. https://doi.org/10.1038/s41576-018-0059-1.

55. Stenson, P.D., Mort, M., Ball, E.V., Chapman, M., Evans, K., Azevedo, L., Hayden, M., Heywood, S., Millar, D.S., Phillips, A.D., and Cooper, D.N. (2020). The Human Gene Mutation Database (HGMD(®)): optimizing its use in a clinical diagnostic or research setting. Hum. Genet. *139*, 1197–1207. https://doi.org/10.1007/s00439-020-02199-3.

56. Özgü, R.K., Durukan, H., Turan, A., Öner, C., Öğüş, A., and Farber, D.B. (2004). Molecular analysis of the ABCA4 gene in Turkish patients with Stargardt disease and retinitis pigmentosa. Hum. Mutat. *23*, 523. https://doi.org/10.1002/humu.9236.

57. Lewis, R.A., Shroyer, N.F., Singh, N., Allikmets, R., Hutchinson, A., Li, Y., Lupski, J.R., Leppert, M., and Dean, M. (1999). Genotype/Phenotype analysis of a photoreceptor-specific ATP-binding cassette transporter gene, ABCR, in Stargardt disease. Am. J. Hum. Genet. *64*, 422–434. https://doi.org/10.1086/302251.

58. Allikmets, R., Singh, N., Sun, H., Shroyer, N.F., Hutchinson, A., Chidambaram, A., Gerrard, B., Baird, L., Stauffer, D., Peiffer, A., et al. (1997). A photoreceptor cell-specific ATP-binding transporter gene (ABCR) is mutated in recessive Stargardt macular dystrophy. Nat. Genet. *15*, 236–246. https://doi.org/10.1038/ng0397-236.

59. Jaakson, K., Zernant, J., Külm, M., Hutchinson, A., Tonisson, N., Glavač, D., Ravnik-Glavač, M., Hawlina, M., Meltzer, M.R., Caruso, R.C., et al. (2003). Genotyping Microarray (Gene Chip) for the ABCR (ABCA4) Gene. Hum. Mutat. *22*, 395–403. https://doi.org/10.1002/humu.10263.

60. Fujinami, K., Lois, N., Davidson, A.E., Mackay, D.S., Hogg, C.R., Stone, E.M., Tsunoda, K., Tsubota, K., Bunce, C., Robson, A.G., et al. (2013). A longitudinal study of Stargardt disease: Clinical and electrophysiologic assessment, progression, and genotype correlations. Am. J. Ophthalmol. *155*, 1075–1088.e13. https://doi.org/10.1016/j.ajo.2013.01.018.

61. Domingo-Prim, J., Riera, M., Abad-Morales, V., Ruiz-Nogales, S., Corcostegui, B., and Pomares, E. (2019). Generation of Best disease-derived induced pluripotent stem cell line (FRIMOi006-A) carrying a novel dominant mutation in BEST1 gene. Stem Cell Res. *40*, 101570. https://doi.org/10.1016/j.scr.2019.101570.

62. Domingo-Prim, J., Abad-Morales, V., Riera, M., Navarro, R., Corcostegui, B., and Pomares, E. (2019). Generation of an induced pluripotent stem cell line (FRIMOi007-A) derived from an incomplete achromatopsia patient carrying a novel homozygous mutation in PDE6C gene. Stem Cell Res. *40*, 101569. https://doi.org/10.1016/j.scr.2019.101569.

63. Riera, M., Navarro, R., Ruiz-Nogales, S., Méndez, P., Burés-Jelstrup, A., Corcóstegui, B., and Pomares, E. (2017). Whole exome sequencing using Ion Proton system enables reliable genetic diagnosis of inherited retinal dystrophies. Sci. Rep. *7*, 42078. https://doi.org/10.1038/srep42078.

64. Domingo-Prim, J., Riera, M., Burés-Jelstrup, A., Corcostegui, B., and Pomares, E. (2019). Establishment of an induced pluripotent stem cell line (FRIMOi005-A) derived from a retinitis pigmentosa patient carrying a dominant mutation in RHO gene. Stem Cell Res. *38*, 101468. https://doi.org/10.1016/j.scr.2019.101468.

65. Riera, M., Patel, A., Corcostegui, B., Chang, S., Corneo, B., Sparrow, J.R., and Pomares, E. (2019). Generation of an induced pluripotent stem cell line (FRIMOi002-A) from a retinitis pigmentosa patient carrying compound heterozygous mutations in USH2A gene. Stem Cell Res. *35*, 101386. https://doi.org/10.1016/j.scr.2019.101386.

66. Okamoto, S., Amaishi, Y., Maki, I., Enoki, T., and Mineno, J. (2019). Highly efficient genome editing for single-base substitutions using optimized ssODNs with Cas9-RNPs. Sci. Rep. *9*, 4811. https://doi.org/10.1038/s41598-019-41121-4.

67. Simkin, D., Papakis, V., Bustos, B.I., Ambrosi, C.M., Ryan, S.J., Baru, V., Williams, L.A., Dempsey, G.T., McManus, O.B., Landers, J.E., et al. (2022). Homozygous might be hemizygous: CRISPR/Cas9 editing in iPSCs results in detrimental on-target defects that escape standard quality controls. Stem Cell Rep. *17*, 993–1008. https://doi.org/10.1016/j.stemcr.2022.02.008.

68. Siles, L., Ruiz-Nogales, S., Navinés-Ferrer, A., Méndez-Vendrell, P., and Pomares, E. (2023). Efficient correction of ABCA4 variants by CRISPR-Cas9 in hiPSCs derived from Stargardt disease patients. Mol. Ther. Nucleic Acids *32*, 64–79. https://doi.org/10.1016/j.omtn.2023.02.032.

69. Siles, L., Gaudó, P., and Pomares, E. (2023). High-Efficiency CRISPR/Cas9-Mediated Correction of a Homozygous Mutation in Achromatopsia-Patient-Derived iPSCs. Int. J. Mol. Sci. *24*, 3655. https://doi.org/10.3390/ijms24043655.

70. Veres, A., Gosis, B.S., Ding, Q., Collins, R., Ragavendran, A., Brand, H., Erdin, S., Cowan, C.A., Talkowski, M.E., and Musunuru, K. (2014). Low incidence of Off-target mutations in individual CRISPR-Cas9 and TALEN targeted human stem cell clones detected by whole-genome sequencing. Cell Stem Cell *15*, 27–30. https://doi.org/10.1016/j.stem.2014.04.020.

71. Yu, W., Lescale, C., Babin, L., Bedora-Faure, M., Lenden-Hasse, H., Baron, L., Demangel, C., Yelamos, J., Brunet, E., and Deriano, L. (2020). Repair of G1 induced DNA double-strand breaks in S-G2/M by alternative NHEJ. Nat. Commun. *11*, 5239. https://doi.org/10.1038/s41467-020-19060-w.

72. Marmorstein, A.D., Kinnick, T.R., Stanton, J.B., Johnson, A.A., Lynch, R.M., and Marmorstein, L.Y. (2015). Bestrophin-1 influences transepithelial electrical properties and Ca2+signaling in human retinal pigment epithelium. Mol. Vis. *21*, 347–359.

73. Regent, F., Morizur, L., Lesueur, L., Habeler, W., Plancheron, A., Ben M'Barek, K., and Monville, C. (2019). Automation of human pluripotent stem cell differentiation toward retinal pigment epithelial cells for large-scale productions. Sci. Rep. *9*, 10646. https://doi.org/10.1038/s41598-019-47123-6.

74. Mazzoni, F., Safa, H., and Finnemann, S.C. (2014). Understanding photoreceptor outer segment phagocytosis: Use and utility of RPE cells in culture. Exp. Eye Res. *126*, 51–60. https://doi.org/10.1016/j.exer.2014.01.010.

75. Kaemmerer, E., Schutt, F., Krohne, T.U., Holz, F.G., and Kopitz, J. (2007). Effects of lipid peroxidation-related protein modifications on RPE lysosomal functions and POS phagocytosis. Investig. Ophthalmol. Vis. Sci. *48*, 1342–1347. https://doi.org/10.1167/iovs.06-0549.

76. Dalvi, S., Galloway, C.A., Winschel, L., Hashim, A., Soto, C., Tang, C., MacDonald, L.A., and Singh, R. (2019). Environmental stress impairs photoreceptor outer segment (POS) phagocytosis and degradation and induces autofluorescent material accumulation in hiPSC-RPE cells. Cell Death Dis. *5*, 96. https://doi.org/10.1038/s41420-019-0171-9.

77. Verosloff, M.S., Shapiro, S.J., Hawkins, E.M., Alpay, E., Verma, D., Stanfield, E.G., Kreindler, L., Jain, S., McKay, B., Hubbell, S.A., et al. (2022). CRISPR-Cas enzymes: The toolkit revolutionizing diagnostics. Biotechnol. J. *17*, e2100304. https://doi.org/10.1002/biot.202100304.

78. Li, C., Chu, W., Gill, R.A., Sang, S., Shi, Y., Hu, X., Yang, Y., Zaman, Q.U., and Zhang, B. (2023). Computational tools and resources for CRISPR/Cas genome editing. Genom. Proteom. Bioinform. *21*, 108–126. https://doi.org/10.1016/j.gpb.2022.02.006.

79. Deng, X., Osikpa, E., Yang, J., Oladeji, S.J., Smith, J., Gao, X., and Gao, Y. (2023). Structural basis for the activation of a compact CRISPR-Cas13 nuclease. Nat. Commun. *14*, 5845. https://doi.org/10.1038/s41467-023-41501-5.

80. Xu, X., Duan, D., and Chen, S.J. (2017). CRISPR-Cas9 cleavage efficiency correlates strongly with targetsgRNA folding stability: From physical mechanism to off-target assessment. Sci. Rep. *7*, 143. https://doi.org/10.1038/s41598-017-00180-1.

81. Liu, X., Homma, A., Sayadi, J., Yang, S., Ohashi, J., and Takumi, T. (2016). Sequence features associated with the cleavage efficiency of CRISPR/Cas9 system. Sci. Rep. *6*, 19675. https://doi.org/10.1038/srep19675.

82. Shams, F., Bayat, H., Mohammadian, O., Mahboudi, S., Vahidnezhad, H., Soosanabadi, M., and Rahimpour, A. (2022). Advance trends in targeting homology-directed repair for accurate gene editing: An inclusive review of small molecules and modified CRISPR-Cas9 systems. Bioimpacts *12*, 371–391. https://doi.org/10.34172/bi.2022.23871.

83. Jensen, K.T., Fløe, L., Petersen, T.S., Huang, J., Xu, F., Bolund, L., Luo, Y., and Lin, L. (2017). Chromatin accessibility and guide sequence secondary structure affect CRISPR-Cas9 gene editing efficiency. FEBS Lett. *591*, 1892–1901. https://doi.org/10.1002/1873-3468.12707.

84. Chung, C.H., Allen, A.G., Sullivan, N.T., Atkins, A., Nonnemacher, M.R., Wigdahl, B., and Dampier, W. (2020). Computational Analysis Concerning the Impact of DNA Accessibility on CRISPR-Cas9 Cleavage Efficiency. Mol. Ther. *28*, 19–28. https://doi.org/10.1016/j.ymthe.2019.10.008.

85. Nambiar, T.S., Billon, P., Diedenhofen, G., Hayward, S.B., Taglialatela, A., Cai, K., Huang, J.W., Leuzzi, G., Cuella-Martin, R., Palacios, A., et al. (2019). Stimulation

of CRISPR-mediated homology-directed repair by an engineered RAD18 variant. Nat. Commun. *10*, 3395. https://doi.org/10.1038/s41467-019-11105-z.

86. Gallagher, D.N., Pham, N., Tsai, A.M., Janto, N.V., Choi, J., Ira, G., and Haber, J.E. (2020). A Rad51-independent pathway promotes single-strand template repair in gene editing. PLoS Genet. *16*, e1008689. https://doi.org/10.1371/journal.pgen.1008689.

87. Shin, H.Y., Wang, C., Lee, H.K., Yoo, K.H., Zeng, X., Kuhns, T., Yang, C.M., Mohr, T., Liu, C., and Hennighausen, L. (2017). CRISPR/Cas9 targeting events cause complex deletions and insertions at 17 sites in the mouse genome. Nat. Commun. *8*, 15464. https://doi.org/10.1038/ncomms15464.

88. Weisheit, I., Kroeger, J.A., Malik, R., Klimmt, J., Crusius, D., Dannert, A., Dichgans, M., and Paquet, D. (2020). Detection of Deleterious On-Target Effects after HDR-Mediated CRISPR Editing. Cell Rep. *31*, 107689. https://doi.org/10.1016/j.celrep.2020.107689.

89. Kosicki, M., Allen, F., Steward, F., Tomberg, K., Pan, Y., and Bradley, A. (2022). Cas9-induced large deletions and small indels are controlled in a convergent fashion. Nat. Commun. *13*, 3422. https://doi.org/10.1038/s41467-022-30480-8.

90. Shen, M.W., Arbab, M., Hsu, J.Y., Worstell, D., Culbertson, S.J., Krabbe, O., Cassa, C.A., Liu, D.R., Gifford, D.K., and Sherwood, R.I. (2018). Predictable and precise template-free CRISPR editing of pathogenic variants. Nature *563*, 646–651. https://doi.org/10.1038/s41586-018-0686-x.

91. Sürün, D., Schwäble, J., Tomasovic, A., Ehling, R., Stein, S., Kurrle, N., von Melchner, H., and Schnütgen, F. (2018). High Efficiency Gene Correction in Hematopoietic Cells by Donor-Template-Free CRISPR/Cas9 Genome Editing. Mol. Ther. Nucleic Acids *10*, 1–8. https://doi.org/10.1016/j.omtn.2017.11.001.

92. Grajcarek, J., Monlong, J., Nishinaka-Arai, Y., Nakamura, M., Nagai, M., Matsuo, S., Lougheed, D., Sakurai, H., Saito, M.K., Bourque, G., and Woltjen, K. (2019). Genome-wide microhomologies enable precise template-free editing of biologically relevant deletion mutations. Nat. Commun. *10*, 4856. https://doi.org/10.1038/s41467-019-12829-8.

93. Nakade, S., Tsubota, T., Sakane, Y., Kume, S., Sakamoto, N., Obara, M., Daimon, T., Sezutsu, H., Yamamoto, T., Sakuma, T., and Suzuki, K.i.T. (2014). Microhomology-mediated end-joining-dependent integration of donor DNA in cells and animals using TALENs and CRISPR/Cas9. Nat. Commun. *5*, 5560. https://doi.org/10.1038/ncomms6560.

94. Navinés-Ferrer, A., Ruiz-Nogales, S., Navarro, R., and Pomares, E. (2022). Impaired Bestrophin Channel Activity in an iPSC-RPE Model of Best Vitelliform Macular Dystrophy (BVMD) from an Early Onset Patient Carrying the P77S Dominant Mutation. Int. J. Mol. Sci. *23*, 7432. https://doi.org/10.3390/ijms23137432.

95. Ameri, H. (2018). Prospect of retinal gene therapy following commercialization of voretigene neparvovec-rzyl for retinal dystrophy mediated by RPE65 mutation. J. Curr. Ophthalmol. *30*, 1–2. https://doi.org/10.1016/j.joco.2018.01.006.

96. Collin, R.W., Den Hollander, A.I., Der Velde-Visser, S.D.V., Bennicelli, J., Bennett, J., and Cremers, F.P. (2012). Antisense oligonucleotide (AON)-based therapy for leber congenital amaurosis caused by a frequent mutation in CEP290. Mol. Ther. Nucleic Acids *1*, e14. https://doi.org/10.1038/mtna.2012.3.

97. Sahel, J.A., Boulanger-Scemama, E., Pagot, C., Arleo, A., Galluppi, F., Martel, J.N., Esposti, S.D., Delaux, A., de Saint Aubert, J.B., de Montleau, C., et al. (2021). Partial recovery of visual function in a blind patient after optogenetic therapy. Nat. Med. *27*, 1223–1229. https://doi.org/10.1038/s41591-021-01351-4.

98. Girach, A., Audo, I., Birch, D.G., Huckfeldt, R.M., Lam, B.L., Leroy, B.P., Michaelides, M., Russell, S.R., Sallum, J.M.F., Stingl, K., et al. (2022). RNA-based therapies in inherited retinal diseases. Therapeutic Advances in Ophthalmology *14*, 25158414221134602. https://doi.org/10.1177/25158414221134602.

99. Liu, Y., Zong, X., Cao, W., Zhang, W., Zhang, N., and Yang, N. (2024). Gene Therapy for Retinitis Pigmentosa: Current Challenges and New Progress. Biomolecules *14*, 903. https://doi.org/10.3390/biom14080903.

100. Scalabrino, M.L., Thapa, M., Wang, T., Sampath, A.P., Chen, J., and Field, G.D. (2023). Late gene therapy limits the restoration of retinal function in a mouse model of retinitis pigmentosa. Nat. Commun. *14*, 8256. https://doi.org/10.1038/s41467-023-44063-8.

101. Jain, R., and Daigavane, S. (2024). Advances and Challenges in Gene Therapy for Inherited Retinal Dystrophies: A Comprehensive Review. Cureus *16*, e69895. https://doi.org/10.7759/cureus.69895.

102. Takagi, S., Mandai, M., Gocho, K., Hirami, Y., Yamamoto, M., Fujihara, M., Sugita, S., Kurimoto, Y., and Takahashi, M. (2019). Evaluation of Transplanted Autologous Induced Pluripotent Stem Cell-Derived Retinal Pigment Epithelium in Exudative Age-Related Macular Degeneration. Ophthalmology Retina *3*, 850–859. https://doi.org/10.1016/j.oret.2019.04.021.

103. Schwartz, S.D., Tan, G., Hosseini, H., and Nagiel, A. (2016). Subretinal transplantation of embryonic stem cell–derived retinal pigment epithelium for the treatment of macular degeneration: An assessment at 4 years. Investig. Ophthalmol. Vis. Sci. *57*, ORSFc1–ORSFc9. https://doi.org/10.1167/iovs.15-18681.

104. Riera, M., Patel, A., Corcostegui, B., Chang, S., Sparrow, J.R., Pomares, E., and Corneo, B. (2019). Establishment and characterization of an iPSC line (FRIMOi001-A) derived from a retinitis pigmentosa patient carrying PDE6A mutations. Stem Cell Res. *35*, 101385. https://doi.org/10.1016/j.scr.2019.101385.

105. Riera, M., Patel, A., Burés-Jelstrup, A., Corcostegui, B., Chang, S., Pomares, E., Corneo, B., and Sparrow, J.R. (2019). Generation of two iPS cell lines (FRIMOi003-A and FRIMOi004-A) derived from Stargardt patients carrying ABCA4 compound heterozygous mutations. Stem Cell Res. *36*, 101389. https://doi.org/10.1016/j.scr.2019.101389.

106. Bae, S., Park, J., and Kim, J.S. (2014). Cas-OFFinder: A fast and versatile algorithm that searches for potential off-target sites of Cas9 RNA-guided endonucleases. Bioinformatics *30*, 1473–1475. https://doi.org/10.1093/bioinformatics/btu048.

107. Gonzalez-Cordero, A., Kruczek, K., Naeem, A., Fernando, M., Kloc, M., Ribeiro, J., Goh, D., Duran, Y., Blackford, S.J.I., Abelleira-Hervas, L., et al. (2017). Recapitulation of Human Retinal Development from Human Pluripotent Stem Cells Generates Transplantable Populations of Cone Photoreceptors. Stem Cell Rep. *9*, 820–837. https://doi.org/10.1016/j.stemcr.2017.07.022.

108. de Bruijn, S.E., Fiorentino, A., Ottaviani, D., Fanucchi, S., Melo, U.S., Corral-Serrano, J.C., Mulders, T., Georgiou, M., Rivolta, C., Pontikos, N., et al. (2020). Structural Variants Create New Topological-Associated Domains and Ectopic Retinal Enhancer-Gene Contact in Dominant Retinitis Pigmentosa. Am. J. Hum. Genet. *107*, 802–814. https://doi.org/10.1016/j.ajhg.2020.09.002.

109. Barnea-Cramer, A.O., Wang, W., Lu, S.-J., Singh, M.S., Luo, C., Huo, H., McClements, M.E., Barnard, A.R., MacLaren, R.E., and Lanza, R. (2016). Function of human pluripotent stem cell-derived photoreceptor progenitors in blind mice. Sci. Rep. *6*, 29784. https://doi.org/10.1038/srep29784.

110. Parinot, C., Rieu, Q., Chatagnon, J., Finnemann, S.C., and Nandrot, E.F. (2014). Large-scale purification of porcine or bovine photoreceptor outer segments for phagocytosis assays on retinal pigment epithelial cells. J. Vis. Exp. 52100. https://doi.org/10.3791/52100.